Preference-Guided Diffusion for Multi-Objective Offline Optimization

Yashas Annadani* 1,3 Syrine Belakaria Stefano Ermon Stefan Bauer 1,3 Barbara Engelhardt 2,4

1 TU Munich Stanford University 3 Helmholtz AI, Munich 4 Gladstone Institutes

Abstract

Offline multi-objective optimization aims to identify Pareto-optimal solutions given a dataset of designs and their objective values. In this work, we propose a preference-guided diffusion model that generates Pareto-optimal designs by leveraging a classifier-based guidance mechanism. Our guidance classifier is a preference model trained to predict the probability that one design dominates another, directing the diffusion model toward optimal regions of the design space. Crucially, this preference model generalizes beyond the training distribution, enabling the discovery of Pareto-optimal solutions outside the observed dataset. We introduce a novel diversity-aware preference guidance, augmenting Pareto dominance preference with diversity criteria. This ensures that generated solutions are optimal and well-distributed across the objective space, a capability absent in prior generative methods for offline multi-objective optimization. We evaluate our approach on various continuous offline multi-objective optimization tasks and find that it consistently outperforms other inverse/generative approaches while remaining competitive with forward/ surrogate-based optimization methods. Our results highlight the effectiveness of classifier-guided diffusion models in generating diverse and high-quality solutions that approximate the Pareto front well.

1 Introduction

Several design problems in science and engineering require optimizing a black-box, expensive-to-evaluate function. For example, in antibiotic drug discovery, the goal is to identify novel molecules with high antibacterial activity [39]. This can be formulated as a single-objective optimization problem. However, in practice, most real-world design challenges involve balancing multiple conflicting objectives. For example, in drug discovery, in addition to maximizing antibacterial activity, we also want to minimize toxicity and production costs [38]. This constitutes a multi-objective experimental design problem.

Prior work in both single and multi-objective optimization (MOO) has largely focused on adaptive experimental design using online methods such as Bayesian optimization [33]. These approaches rely on training surrogate models for each objective function and designing acquisition functions that are typically optimized via gradient-based techniques [3] or evolutionary algorithms to determine the next candidate for evaluation. This process is iteratively repeated to optimize the objectives. However, in many real-world applications, sequential evaluations—where inputs are tested one at a time or in small batches—are impractical. In some cases, we have only a single opportunity to evaluate the function, and we must allocate the entire evaluation budget efficiently.

^{*}Correspondence to yashas.annadani@gmail.com. Code available at https://github.com/yannadani/pgd_moo.

For example, in drug design, scientists cannot test molecules one by one in wet lab experiments due to the high cost, slow turnaround, and the inherently parallelizable nature of the process [38]. Instead, it is common to evaluate all candidate molecules in a single batch. This setting is referred to as offline black-box optimization [41]. While recent work has explored offline optimization in the single-objective setting [23, 46], where extensive prior data is leveraged to model the objective function and identify potential optima, the MO case remains relatively underexplored.

Offline black-box optimization presents distinct challenges compared to traditional online optimization. Since the algorithm cannot iteratively refine the learned model using newly acquired data, it must effectively leverage the available dataset to generalize beyond observed data points. This is particularly challenging because the true optima are often expected to lie outside the existing dataset, requiring robust extrapolation. Additionally, the goal is not merely to identify data points with high function values but to find solutions that satisfy a well-defined notion of optimality, such as the *Pareto* optimality.

Prior work in single-objective offline optimization can generally be categorized into two main approaches: forward and inverse methods. Forward approaches attempt to mimic strategies used in online optimization while leveraging offline data [41]. These methods train a surrogate model of the objective function and optimize it using gradient-based techniques to propose a set of promising inputs for evaluation. They are effective when the search space is well-defined. In contrast, inverse approaches use generative models to learn an inverse mapping from function values to inputs, enabling the generation of new candidates with potentially high objective values [6, 16, 24, 25]. This distinction is critical when optimal inputs are not known in advance. For example, in chemistry, if the goal is to evaluate a known molecule, surrogate models are effective in predicting its properties. However, if the goal is to discover entirely new molecules with desired properties, inverse methods are essential, as they directly generate novel candidates rather than selecting from a predefined space. Some generative modeling approaches also draw inspiration from online methods by constructing synthetic optimization trajectories from offline data, aiming to generate new optimal points by extrapolating from the learned trajectories [23].

Multi-objective offline optimization introduces additional challenges beyond those encountered in the single-objective setting. In single-objective optimization, the goal is simply to maximize (or minimize) a function value. However, in the multi-objective case, we seek to achieve best trade-offs among competing objectives, which is formalized by Pareto optimality. Beyond identifying Pareto-optimal solutions, another critical challenge is ensuring diversity on the Pareto front. A well-structured Pareto front should provide solutions spread across different regions of the objective space, representing a broad range of Pareto-optimal designs. Although the problem of ensuring diversity of solutions is addressed in online MOO [1], ensuring both optimality and diversity is challenging in the offline setting as the algorithm must infer these solutions solely from existing data.

Xue et al. [45] has recently explored benchmarking offline multi-objective optimization (MOO) by building offline datasets for a variety of MOO benchmarks and proposing several potential algorithms. Their work extends some offline single-objective optimization (SOO) approaches to the MOO setting, such as fitting surrogate models to the offline data and optimizing over the surrogates using evolutionary algorithms. However, this work has not explored the possibility of using generative models for offline MOO.

Our contributions are:

- We formulate offline MOO as an inverse problem, and propose a novel algorithm based on diffusion models with preference-based classifier guidance. This classifier is trained to compare two candidate designs and determine which is more likely to dominate the other in the objective space.
- We address the diversity challenge in the offline MOO setting. Rather than just identifying high-value designs, we train the preference model to favor solutions that are not only optimal but also well-distributed across the objective space.
- We demonstrate through extensive experiments on both synthetic and real-world settings that our approach performs better than other inverse methods in terms of convergence to the Pareto front and the diversity of obtained solutions.
- Among inverse techniques, our approach consistently achieves the strongest results; making it a competitive choice in cases where forward methods are not feasible. Even when forward

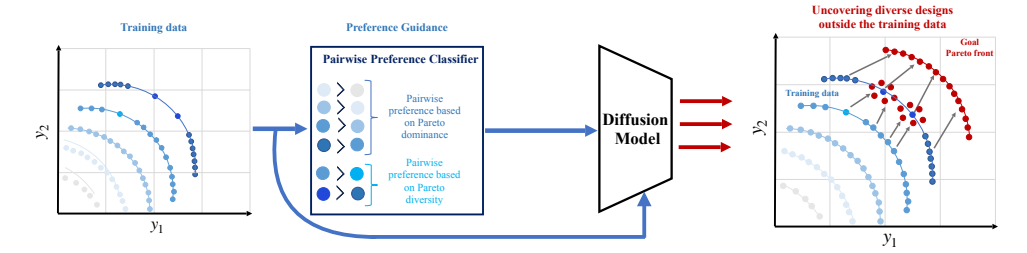


Figure 1: A schematic representation of the proposed preference guided diffusion approach for offline multiobjective optimization.

methods are applicable, our algorithm remains competitive while maintaining the benefits of generative exploration.

2 Background

2.1 Offline Multi-Objective Optimization

Multi-objective optimization (MOO) seeks to find the design $x \in \mathcal{X}^d$ that minimizes (or maximizes) a set of m different objectives:

$$\min_{\boldsymbol{x} \in \mathcal{X}^d} \boldsymbol{f}(\boldsymbol{x}) \coloneqq \{f_1(\boldsymbol{x}), \dots, f_m(\boldsymbol{x})\},\tag{1}$$

where $f_i: \mathcal{X}^d \mapsto \mathbb{R}$ is an unknown and expensive-to-evaluate objective. For most practical problems, the objectives are not simultaneously optimizable by a single design. Hence, the goal instead is to find the set of designs that are *Pareto optimal*.

Definition 2.1 (Pareto Dominance). A design x *Pareto dominates* another design $z \in \mathcal{X}^d$ (denoted by $x \prec z$) if $f_i(x) \leq f_i(z) \ \forall i$ and $\exists j : f_j(x) < f_j(z)$.

Definition 2.2 (Pareto Optimality and Pareto Front). A design x^* is *Pareto optimal* if $\nexists x \in \mathcal{X}^d$ such that $x \prec x^*$. The set of all Pareto optimal designs is called a *Pareto set*. Correspondingly, the objective values of the Pareto set $\{f(x^*) \mid x^*\}$ is called the *Pareto front (PF)*.

The Pareto front provides an optimal set of trade-offs that can be achieved from the objectives when they are not simultaneously optimizable.

Sequential methods that collect data by selecting designs and evaluating their function values are the most common approach for MOO, making use of surrogate models with uncertainty quantification to learn the unknown objectives. However, for many practical problems, these sequential methods are not feasible due to prohibitive cost or time constraints (or both). Instead of iteratively allocating an evaluation budget to refine the design choices, offline optimization uses the entire budget in a single round of function evaluations. In offline optimization, we have access to a dataset of N non-optimal design-objective values pairs $\mathcal{D} := \{(\boldsymbol{x}^{(i)}, f(\boldsymbol{x}^{(i)})\}_{i=1}^{N}$. The goal of offline MOO is to find the Pareto-optimal set by relying only on the existing dataset \mathcal{D} .

2.2 Diffusion Models

Diffusion models [17, 34, 35] are a class of generative models defined by a Markov chain that sequentially adds noise to data samples and then learns to denoise from white noise (i.e., generate a sample) by reversing the Markov chain. In this work, we follow the Denoising Diffusion Probabilistic Models (DDPM) [17] approach, which we summarize here. Given a sample $x_0 \sim q(x)$, a time-dependent forward noising process is defined as:

$$q(\boldsymbol{x}_t \mid \boldsymbol{x}_{t-1}) := \mathcal{N}(\boldsymbol{x}_t; \sqrt{1 - \beta_t} \boldsymbol{x}_{t-1}, \beta_t \mathbb{I}_d), \tag{2}$$

where β_t is the variance of the noising schedule at timestep t such that $\beta_1 < \beta_2 < \cdots < \beta_T$, and T is the total number of timesteps. Let $\alpha_t = 1 - \beta_t$ and $\tilde{\alpha}_t = \prod_{i=1}^t \alpha_i$; then the noised sample \boldsymbol{x}_t can

be obtained in closed form:

$$\mathbf{x}_t = \sqrt{\tilde{\alpha}_t} \mathbf{x}_0 + \sqrt{1 - \tilde{\alpha}_t} \epsilon_t, \quad \epsilon_t \sim \mathcal{N}(0, \mathbb{I}_d).$$
 (3)

The reverse process conditional $q(\boldsymbol{x}_{t-1} \mid \boldsymbol{x}_t)$ is not tractable. Therefore, a denoising model defined as $p_{\theta}(\boldsymbol{x}_{t-1} \mid \boldsymbol{x}_t) \coloneqq \mathcal{N}(\boldsymbol{x}_{t-1}; \mu_{\theta}(\boldsymbol{x}_t), \Sigma_{\theta}(\boldsymbol{x}_t))$ is learned by optimizing parameters θ . Instead of parameterizing the reverse process to estimate $\mu_{\theta}(\boldsymbol{x}_t)$, it is common to reparameterize this reverse process to predict the noise that was added to produce \boldsymbol{x}_t (equation 3). If $\epsilon_{\theta}(\boldsymbol{x}_t, t)$ is the denoising model to predict the added noise, reparameterization yields the mean $\mu_{\theta}(\boldsymbol{x}_t)$ as:

$$\mu_{\theta}(\boldsymbol{x}_t) = \frac{1}{\sqrt{\alpha_t}} \left(\boldsymbol{x}_t - \frac{1 - \alpha_t}{\sqrt{1 - \tilde{\alpha}_t}} \epsilon_{\theta}(\boldsymbol{x}_t, t) \right). \tag{4}$$

The reverse process variance is set to be the same as the forward process variance at time t, i.e., $\Sigma_{\theta}(x_t) := \beta_t \mathbb{I}_d$. The denoising model can be trained with mean squared error (MSE) loss:

$$\ell(\theta) = \mathbb{E}_{t,\epsilon_t, \mathbf{x}_0} \left[\|\epsilon_t - \epsilon_\theta(\mathbf{x}_t, t)\|_2^2 \right]. \tag{5}$$

A new sample can be generated by first sampling $\tilde{x}_T \sim \mathcal{N}(0, \mathbb{I}_d)$ and then autoregressively sampling from $\mathcal{N}(x_{t-1}; \mu_{\theta}(\tilde{x}_t), \beta_t \mathbb{I}_d)$ to get \tilde{x}_0 .

2.3 Classifier Guidance

If label o corresponding to each sample x_0 is available, then classifier guidance allows one to generate new samples from a trained diffusion model specific to a desired label. To do this, classifier guidance [13] trains an additional time-dependent classifier of the input $p_{\phi}(o \mid x_t, t)$. Along with the trained denoising model $\epsilon_{\theta}(x_t, t)$, a new conditional sample can be generated by first sampling $\tilde{x}_T \sim \mathcal{N}(0, \mathbb{I}_d)$ and then, from t = T to t = 1, autoregressively sampling:

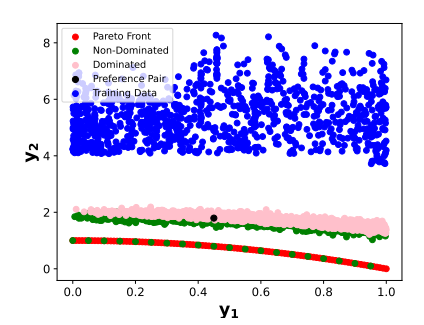
$$\tilde{\boldsymbol{x}}_{t-1} \mid \boldsymbol{o}, \tilde{\boldsymbol{x}}_t \sim \mathcal{N}(\boldsymbol{x}_{t-1}; \mu_{\theta}(\tilde{\boldsymbol{x}}_t) + w\beta_t \nabla_{\tilde{\boldsymbol{x}}_t} \log p_{\phi}(\boldsymbol{o} \mid \tilde{\boldsymbol{x}}_t, t), \beta_t \mathbb{I}_d),$$
 (6)

where w is the *guidance strength*. In this work, we use classifier guidance to generate samples that approximate the optimal Pareto sets where the classifier is a preference model that predicts the dominance of one input over the other.

3 Related Work

Online Multi-Objective Black-Box Optimization: Adaptive experimental design has primarily explored multi-objective optimization (MOO) in an online or sequential fashion, where solutions are iteratively refined as new data arrives [1, 4]. Although less studied than single-objective optimization, several sequential approaches have proven effective. The most established is Bayesian optimization (BO) [18, 33], which typically uses Gaussian processes [44] to model objectives, especially in data-scarce regimes. Multi-objective extensions of BO often reduce the problem via scalarization [21] or employ acquisition functions such as expected hypervolume improvement (EHVI) [15] and information gain [4] to balance trade-offs across objectives. Recent work also introduced batch selection strategies [11], though most methods emphasize Pareto dominance over diversity. A few exceptions, such as Konakovic Lukovic et al. [22] and Ahmadianshalchi et al. [1], explicitly promote Pareto front diversity. Beyond traditional BO, neural approaches extend online MOO using generative models like variational autoencoders (VAEs) combined with Gaussian processes over the latent space [36]. However, these methods inherit VAE limitations—posterior collapse and non-identifiability—that restrict their robustness in practical optimization tasks.

Offline Single-Objective Black-Box Optimization: Offline single-objective optimization focuses on leveraging existing datasets without additional data collection. Forward methods [41, 46] train surrogate models to approximate the objective function and then optimize these surrogates for high-performing inputs. Inverse methods instead employ conditional GANs [6, 16, 25] to learn mappings from function outputs back to inputs. To bridge forward and inverse strategies, Chemingui et al. [7], Krishnamoorthy et al. [23] proposed hybrid methods that synthesize pseudo-optimization trajectories from offline data, mimicking online behavior. Diffusion-based frameworks [24] adjust diffusion losses with weighted importance terms, while classifier-guided models [8] bias generation toward globally optimal designs. Kim et al. [19] provides a comprehensive review of model-based offline optimization methods, summarizing progress across forward, inverse, and hybrid approaches. Additionally, Trabucco et al. [42] established a standardized benchmarking suite for consistent evaluation of offline optimization algorithms.



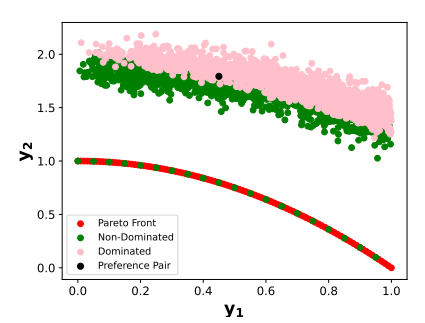


Figure 2: Generalization of the preference model on regions unseen in the training data on the ZDT2 task [53]. The preference model gives good prediction of Pareto dominance between the reference design (in black) with other designs (in pink and green). Pink indicates that the preference model predicts these designs to be dominated by the reference design and green indicates that these designs are predicted as dominating the reference design. The figure on the right is a zoomed-in version of the left, excluding the training data (in blue).

Offline Multi-Objective Black-Box Optimization: Research on offline multi-objective optimization (MOO) remains limited. Xue et al. [45] recently proposed a benchmarking framework with offline datasets and baseline algorithms across MOO benchmarks. Their work mainly extends forward-style single-objective methods by fitting surrogate models to offline data and optimizing them via evolutionary algorithms but does not explore generative or inverse techniques. Concurrently, Yuan et al. [48] introduced ParetoFlow, a flow-based generative model for offline MOO that embeds objective weighting directly into the loss function, effectively scalarizing multiple objectives. While this inverse approach is promising, it does not explicitly address Pareto front diversity—an essential factor for capturing representative trade-offs in MOO.

4 Preference-Guided Diffusion for Offline Multi-Objective Optimization

We present a new effective approach for offline MOO by using classifier guidance to generate samples from Pareto optimal sets with a diffusion model trained on offline data. Our approach does not require training individual surrogate models for each objective. It relies on an inverse strategy while ensuring the ability to generate diverse samples from the Pareto optimal set. We refer to our method as *preference-guided diffusion for multi-objective offline optimization* (PGD-MOO).

Let $x \in \mathcal{X}^d \subseteq \mathbb{R}^d$ be any d-dimensional design with corresponding objective values $y_i = f_i(x)$ defined by unknown and expensive-to-evaluate functions $f_i : \mathcal{X}^d \mapsto \mathbb{R}$. Let $y = [y_1, \dots, y_m]^T$ be the vector of objective values for an m-objective problem. In offline MOO, we have access to a dataset $\mathcal{D} := \{x^{(i)}, y^{(i)}\}_{i=1}^N$ of N previously evaluated design-objective pairs. Given \mathcal{D} , the goal is to generate designs x^* from the unknown optimal Pareto set.

While diffusion models capture the distribution over data p(x), in offline MOO, we are often interested in samples that lie outside the training data, closer to the Pareto front. This motivates the use of classifier guidance. Directly using classifier guidance in diffusion models involves training surrogate models for each objective, which often requires scalarization and hence can be suboptimal. We propose to use preference-based guidance to capture Pareto dominance relations between data points.

4.1 Preference Guided Diffusion

In this work, we explore an alternate guidance strategy that does not involve training surrogate models for every objective. Instead, we model the space of multiple-objectives through preference pairs, as defined by a Bradley-Terry model [5] of designs.

In this regard, we train a preference model that predicts the (log)- probability of whether a design Pareto dominates (Definition 2.1) another design. During sampling of the designs, Given two designs x and \hat{x} , we train a (time-conditioned) binary classifier that predicts $\log p_{\phi}(x \prec \hat{x} \mid x, \hat{x}, t)$. We parameterize this distribution with a multi-layer perceptron (MLP) that takes in two inputs (designs) of size $2 \times d$ and outputs the logit of the Bernoulli distribution predicting whether the first input Pareto dominates the second input.

Algorithm 1 Sampling from Preference Guided Diffusion

Require: Trained $\epsilon_{\theta}(\boldsymbol{x}_t,t)$, preference model $p_{\phi}(\boldsymbol{x} \prec \hat{\boldsymbol{x}} \mid \boldsymbol{x}, \hat{\boldsymbol{x}},t)$, guidance weight w and the most dominant design in the dataset $\boldsymbol{x}^{\mathcal{D}(\mathsf{best})}$

```
1: r \leftarrow \boldsymbol{x}^{\mathcal{D}(\text{best})}
2: \tilde{\boldsymbol{x}}_T \sim \mathcal{N}(0, \mathbb{I}_d)
3: for \mathbf{t} = T to 1 do
4: \mu_{\theta}(\tilde{\boldsymbol{x}}_t) = \frac{1}{\sqrt{\alpha_t}} \left( \tilde{\boldsymbol{x}}_t - \frac{1-\alpha_t}{\sqrt{1-\tilde{\alpha}_t}} \epsilon_{\theta}(\tilde{\boldsymbol{x}}_t, t) \right)
5: Compute preference score s_p = \nabla_{\tilde{\boldsymbol{x}}_t} p_{\phi}(\tilde{\boldsymbol{x}}_t \prec r \mid \tilde{\boldsymbol{x}}_t, r, t)
6: Sample \tilde{\boldsymbol{x}}_{t-1} \sim \mathcal{N}(\boldsymbol{x}_{t-1}; \mu_{\theta}(\tilde{\boldsymbol{x}}_t) + w\beta_t s_p, \beta_t \mathbb{I}_d)
7: r \leftarrow \tilde{\boldsymbol{x}}_t
8: end for
9: return \tilde{\boldsymbol{x}}_0
```

Training the Preference Classifier. To train the preference classifier, we first sort the points in the training data by their Pareto dominance. This divides the data into multiple fronts in increasing order of dominance, with points in the same front considered equally dominant. Next, we select (x, \hat{x}) pairs randomly from the dataset. If one design strictly dominates the other, it is labeled as preferred. If both x and \hat{x} are equally dominant, we assign the label $x \prec \hat{x}$ if x has more diversity contribution than \hat{x} wrt other points that belong to the front. The diversity contribution of each point is calculated using the crowding distance [12] of a selected design w.r.t all other points that belong to the same front in the dataset. Crowding distance for any point x is computed as follows:

$$d_{\text{CD}}(\boldsymbol{x}) = \sum_{i=1}^{m} \frac{y_i^+ - y_i^-}{y_i^{\text{max}} - y_i^{\text{min}}},\tag{7}$$

where y_i^+ and y_i^- are the i^{th} objective values of neighboring designs of \boldsymbol{x} in the corresponding front sorted according to ith objective value. y_i^{\max} and y_i^{\min} are the maximum and minimum values of the objective i in the current front. Crowding distance has been used as a secondary selection criterion in evolutionary algorithms such as NSGA-2 [12] to maintain the diversity of solutions. Using crowding distance to create a binary label encourages the preference model to not only guide the diffusion model towards more Pareto-dominant regions, but also ensure that the designs that make up the Pareto front are diverse. For the denoising model, we train an unconditional diffusion model $\epsilon_{\theta}(\boldsymbol{x}_t,t)$ (§2.2) on the designs \boldsymbol{x} in the dataset, similar to DDPM [17].

Sampling Designs. With a trained denoising model $\epsilon_{\theta}(\boldsymbol{x}_{t},t)$ and preference model $p_{\phi}(\boldsymbol{x} \prec \hat{\boldsymbol{x}} \mid \boldsymbol{x},\hat{\boldsymbol{x}},t)$, we sample a new design by using classifier guidance (§2.3). We input both the denoised variable at the current timestep $\tilde{\boldsymbol{x}}_{t}$ as well as from the previous realization of denoising, i.e., $\tilde{\boldsymbol{x}}_{t+1}$ for the preference model to estimate $\nabla_{\tilde{\boldsymbol{x}}_{t}}p_{\phi}(\tilde{\boldsymbol{x}}_{t} \prec \tilde{\boldsymbol{x}}_{t+1} \mid \tilde{\boldsymbol{x}}_{t}, \tilde{\boldsymbol{x}}_{t+1}, t)$. At the beginning of the denoising procedure when \boldsymbol{x}_{t+1} is not defined, we input the most dominant design in the dataset for preference comparison. The most dominant design in the dataset is chosen based on non-dominated sorting. The sampling procedure is summarized in Algorithm 1. Intuitively, a preference model that generalizes well beyond its training data should guide the denoising process such that, at each step of denoising, the resulting sample $\tilde{\boldsymbol{x}}_{t}$ is in a more Pareto-dominant region.

With enough timesteps, the resulting denoised sample \tilde{x}_0 will be close to the Pareto front. Moreover, the connection to Bradley-Terry model of preference is apparent: the gradient of the logit which indicates the probability of the first input dominating the second, carries information about the reward [32]. Here, we use this to guide the diffusion model such that it can sample from regions closer to the Pareto front through the denoising process.

This approach does not require training surrogate models, thus providing a simple alternative approach to offline MOO. We find that the preference model generalizes well outside of the training data (see Fig. 2), therefore providing guidance to the diffusion model to generate designs outside of the training data close to the Pareto front, while maintaining diversity in the samples.

5 Experiments

We perform several experiments on standard benchmarks for offline MOO. Through these experiments, we would like to understand how close the generated samples are to the Pareto front, as well as the diversity of the solutions.

Benchmark Tasks: Our evaluation closely follows the benchmarking effort provided in prior work [45]. We evaluate our approach on two sets of tasks: **synthetic** and real-world applications-based **RE** engineering suite [40]. Each task consists of a dataset of 60k offline datapoints. As in [45], we use 54k randomly chosen data points for training and the remaining for validation.

- 1. Synthetic set of tasks consist of 12 distinct tasks each with their own dataset. The objectives are analytic functions with tractable Pareto-fronts. This set of tasks has been widely used in MOO problems. Every task consists of 2-3 objectives with d ranging from 10 to 30.
- **2. RE** engineering suite of problems are set of 12 distinct tasks, each with their own dataset. These tasks are based on real-world applications in engineering, for instance, rocket injector design and disc brake design. d ranges from 3-7 variables and the number of objectives m varies from 2 to 6.
- **3. MO-NAS** are set of tasks are based on neural architecture search benchmarks from [14, 27, 30] which consists of multiple objectives like prediction error and hardware constraints like GPU latency. In particular, we use the datasets corresponding to C10/MOP(1-9) and IN1K/MOP(1-9) tasks provided by Lu et al. [30]. As the design space is discrete, we operate on the continuous space of corresponding logits, as in prior work [45, 48].

Details of individual tasks and their corresponding datasets are given in Appendix B.

Baselines: We compare our approach with two categories of baselines:

- 1. We compare with **ParetoFlow** [48], a classifier guided generative model based on flow-matching [28]. Classifiers for guidance are trained surrogate models for each objective, followed by scalarization. ParetoFlow is our **primary baseline** since our work is mainly concerned with studying inverse approaches for offline MOO.
- **2.** Forward approaches using evolutionary algorithms: As suggested in prior work [45], a standard approach to offline MOO is to train a surrogate

Table 1: Average ranking of hypervolume obtained by different methods across synthetic, RE and MO-NAS tasks.

Method	Synthetic	RE	MO-NAS
MultiHead	7.5	5.73	10.11
MultiHead - PcGrad	6.08	6.06	8.00
MultiHead - GradNorm	9.75	11.4	8.50
MultipleModels	6.5	3.67	9.39
MultipleModels - COM	7.83	7.27	2.72
MultipleModels - IOM	5.58	4.6	5.44
MultipleModels - ICT	6.67	4.67	6.61
MultipleModels - RoMA	6.58	7.67	7.44
MultipleModels - TriMentoring	8.33	4.3	8.11
ParetoFlow	7.58	6.17	4.67
PGD-MOO + Data Pruning (Ours)	5.08	9.06	2.14
PGD-MOO (Ours)	4.42	7.67	1.86

model for each objective and then use evolutionary algorithms such as NSGA-2 [12] to search over the design space. Although there are various ways to learn surrogate models, we compare with deep neural network (DNN)-based approaches, which are shown to perform best according to benchmarks [45]. The DNN approaches we compare with are: i) **A Multi-Head** Model: Uses multi-task learning [50] to train a joint surrogate for all objectives. Training techniques for this approach such as GradNorm [10] and PcGrad [47] are also compared. ii) **Multiple Models**: Maintain m independent surrogate models, each making use of a single optimization technique, including COMs [41], ROMA [46], IOM [31], ICT [49], and Tri-mentoring [9].

Other forward approaches like multi-objective Bayesian optimization algorithms are shown to perform worse than evolutionary algorithms on both synthetic and RE set of tasks [45], hence we exclude them from comparisons in this work.

Evaluation Metrics: For each algorithm, we evaluate the convergence of solutions using the hypervolume metric [52], a standard metric in MOO for measuring the closeness of the proposed designs to the Pareto front. *Hypervolume* measures the volume of the objective space between a

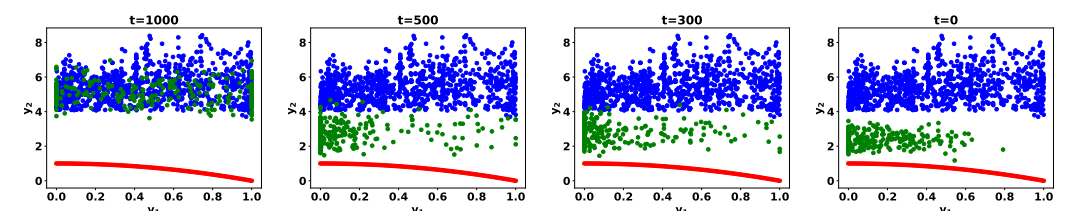


Figure 3: Plot of the samples from our preference-guided diffusion model (in green) on the ZDT2 task [53] at different timesteps of denoising. Convergence of samples close to the Pareto front (in red) outside of the training data (blue) highlights the importance of preference guidance.

Table 2: Hypervolume results of DTLZ subtasks (part of the **synthetic** task). Each method is run for five random seeds and evaluated on 256 designs.

Method	DTLZ1	DTLZ2	DTLZ3	DTLZ4	DTLZ5	DTLZ6	DTLZ7
D (best)	10.60	9.91	10.00	10.76	9.35	8.88	8.56
MultiHead	10.51 ± 0.23	9.03 ± 0.56	10.48 ± 0.23	6.73 ± 1.4	8.41 ± 0.15	8.72 ± 1.07	10.66 ± 0.09
MultiHead - PcGrad	10.64 ± 0.01	9.64 ± 0.33	10.55 ± 0.12	9.95 ± 1.93	9.02 ± 0.24	9.90 ± 0.25	10.61 ± 0.03
MultiHead - GradNorm	$10.64 \pm .01$	8.86 ± 1.27	10.26 ± 0.28	7.45 ± 0.75	7.87 ± 1.06	8.16 ± 2.21	10.31 ± 0.22
MultipleModels	10.64 ± 0.01	9.03 ± 0.80	10.58 ± 0.03	7.66 ± 1.3	7.65 ± 1.39	9.58 ± 0.31	10.61 ± 0.16
MultipleModels - COM	10.64 ± 0.01	8.99 ± 0.97	10.27 ± 0.37	9.72 ± 0.39	9.44 ± 0.41	9.37 ± 0.35	10.09 ± 0.36
MultipleModels - IOM	10.64 ± 0.01	10.10 ± 0.27	10.24 ± 0.13	10.03 ± 0.53	9.77 ± 0.18	9.30 ± 0.31	10.60 ± 0.05
MultipleModels - ICT	10.64 ± 0.01	8.68 ± 0.88	10.25 ± 0.42	10.33 ± 0.24	9.25 ± 0.28	9.10 ± 1.16	10.29 ± 0.05
MultipleModels - RoMA	10.64 ± 0.01	10.04 ± 0.05	10.61 ± 0.03	9.25 ± 0.11	8.71 ± 0.47	9.84 ± 0.25	10.53 ± 0.04
MultipleModels - TriMentoring	10.64 ± 0.01	9.39 ± 0.35	10.48 ± 0.12	10.21 ± 0.06	7.69 ± 1.03	9.00 ± 0.48	10.12 ± 0.09
ParetoFlow	10.60 ± 0.02	10.13 ± 0.16	10.41 ± 0.09	10.29 ± 0.17	9.65 ± 0.23	9.25 ± 0.43	8.94 ± 0.18
PGD-MOO + Data Pruning (Ours)	10.64 ± 0.01	10.55 ± 0.01	10.63 ± 0.01	10.63 ± 0.01	10.07 ± 0.02	10.15 ± 0.03	9.57 ± 0.07
PGD-MOO (Ours)	10.65 ± 0.01	$\textbf{10.55} \pm \textbf{0.01}$	10.63 ± 0.01	$\textbf{10.64} \pm \textbf{0.01}$	$\textbf{10.06} \pm \textbf{0.02}$	$\textbf{10.14} \pm \textbf{0.01}$	9.70 ± 0.18

reference point and the objective vectors of the solution set, and does not require access to the true Pareto front. The reference point used for evaluation of hypervolume is taken from [45](Appendix B).

In addition to the hypervolume, we also measure the diversity of the obtained solutions using the Δ -spread metric [12, 51]. The Δ -spread measures the extent of the spread achieved in a computed Pareto front approximation [2]. It is important to consider the diversity of the obtained solutions, especially in the case of MOO wherein there is no single "best" design, but rather an entire set of solutions based on the Pareto front. In addition, in the case of offline optimization, the acquisition is single-shot. Therefore, solutions that are diverse and hence provide more coverage over the objective space are preferable. In this work, we provide the first effort to evaluate and benchmark the diversity of solutions obtained by different approaches in offline MOO. Further details of the evaluation metrics and their computation is provided in Appendix A.1.

We evaluate all methods on 5 random seeds, and compute the metrics using a budget of 256 designs.

5.1 Training Details

We parameterize the unconditional denoising model to be a multi-layer perceptron (MLP) with two 512-dimensional hidden layers, followed by a ReLU nonlinearity and layer normalization [26]. We also incorporate sinusoidal time embedding [43] for conditioning. We parameterize the preference model to be an MLP with three hidden layers, with first two hidden layers having the same number of units as the input, while the last hidden layer is having 512 units. Similar to denoising model, we also use ReLU nonlinearity followed by layer normalization and sinusoidal time embedding.

The denoising model is trained with AdamW optimizer [29] with learning rate of 5e-4 for up to 200 epochs. Following Ho et al. [17], we employ a linear noise schedule such that the noise β_t grows linearly from 1e-4 to 0.02. The preference model is trained with Adam optimizer [20] with learning rate of 1e-5 for up to 500 epochs. During sampling, we set the guidance weight w to 10. For the preference model, we also experiment with pruning the training data to only contain the top 30% of points, sorted according to their dominance. We refer to this method as **PGD-MOO + Data Pruning** in the results.

Table 3: Hypervolume results of ZDT subtasks (part of the **synthetic** task). Each method is run for five random seeds and evaluated on 256 designs.

Method	ZDT1	ZDT2	ZDT3	ZDT4	ZDT6
D (best)	4.17	4.67	5.15	5.45	4.61
MultiHead	4.8 ± 0.03	5.57 ± 0.07	5.58 ± 0.2	4.59 ± 0.26	4.78 ± 0.01
MultiHead - PcGrad	$\textbf{4.84} \pm \textbf{0.01}$	5.55 ± 0.11	5.51 ± 0.03	3.68 ± 0.70	4.67 ± 0.1
MultiHead - GradNorm	4.63 ± 0.15	5.37 ± 0.17	5.54 ± 0.2	3.28 ± 0.9	3.81 ± 1.2
MultipleModels	4.81 ± 0.02	5.57 ± 0.07	5.48 ± 0.21	5.03 ± 0.19	4.78 ± 0.01
MultipleModels - COM	4.52 ± 0.02	4.99 ± 0.12	5.49 ± 0.07	$\textbf{5.10} \pm \textbf{0.08}$	4.41 ± 0.21
MultipleModels - IOM	4.68 ± 0.12	5.45 ± 0.11	5.61 ± 0.06	4.99 ± 0.21	4.75 ± 0.01
MultipleModels - ICT	4.82 ± 0.01	5.58 ± 0.01	5.59 ± 0.06	4.63 ± 0.43	4.75 ± 0.01
MultipleModels - RoMA	$\textbf{4.84} \pm \textbf{0.01}$	5.43 ± 0.35	$\textbf{5.89} \pm \textbf{0.04}$	4.13 ± 0.11	1.71 ± 0.10
MultipleModels - TriMentoring	4.64 ± 0.10	5.22 ± 0.11	5.16 ± 0.04	$\textbf{5.12} \pm \textbf{0.12}$	2.61 ± 0.01
ParetoFlow	4.23 ± 0.04	$\textbf{5.65} \pm \textbf{0.11}$	5.29 ± 0.14	5.00 ± 0.22	4.48 ± 0.11
PGD-MOO + Data Pruning (Ours)	4.54 ± 0.08	5.21 ± 0.06	5.61 ± 0.06	5.06 ± 0.07	4.56 ± 0.14
PGD-MOO (Ours)	4.41 ± 0.08	5.33 ± 0.05	5.54 ± 0.10	5.02 ± 0.03	$\textbf{4.82} \pm \textbf{0.01}$

Table 4: Selected results of hypervolume on **RE** task. Results are evaluated on 256 designs with five different random seeds.

Method	RE21	RE22	RE25	RE32	RE35	RE37	RE41	RE61
D(best)	4.1	4.78	4.79	10.56	10.08	5.57	18.27	97.49
MultiHead-GradNorm	4.28 ± 0.39	4.7 ± 0.44	4.52 ± 0.5	10.54 ± 0.15	9.76 ± 1.3	5.67 ± 1.41	17.06 ± 3.82	108.01 ± 1.0
MultiHead-PcGrad	4.59 ± 0.01	4.73 ± 0.36	4.78 ± 0.14	10.63 ± 0.01	10.51 ± 0.05	6.68 ± 0.06	20.66 ± 0.1	108.54 ± 0.23
MultiHead	4.6 ± 0.0	$\textbf{4.84} \pm \textbf{0.0}$	4.74 ± 0.2	10.6 ± 0.05	10.49 ± 0.07	6.67 ± 0.05	20.62 ± 0.11	108.92 ± 0.22
MultipleModels-COM	4.38 ± 0.09	$\textbf{4.84} \pm \textbf{0.0}$	4.83 ± 0.01	10.64 ± 0.01	10.55 ± 0.02	6.35 ± 0.1	20.37 ± 0.06	107.99 ± 0.48
MultipleModels-ICT	4.6 ± 0.0	$\textbf{4.84} \pm \textbf{0.0}$	$\textbf{4.84} \pm \textbf{0.0}$	10.64 ± 0.0	10.5 ± 0.01	6.73 ± 0.0	20.58 ± 0.04	108.68 ± 0.27
MultipleModels-IOM	4.58 ± 0.02	4.84 ± 0.0	4.83 ± 0.01	$\textbf{10.65} \pm \textbf{0.0}$	10.57 ± 0.01	6.71 ± 0.02	20.66 ± 0.05	107.71 ± 0.5
MultipleModels-RoMA	4.57 ± 0.0	4.61 ± 0.51	4.83 ± 0.01	10.64 ± 0.0	10.53 ± 0.03	6.67 ± 0.02	20.39 ± 0.09	108.47 ± 0.28
MultipleModels-TriMentoring	4.6 ± 0.0	4.84 ± 0.0	$\textbf{4.84} \pm \textbf{0.0}$	10.62 ± 0.01	10.59 ± 0.0	$\textbf{6.73} \pm \textbf{0.01}$	20.68 ± 0.04	108.61 ± 0.29
MultipleModels	4.6 ± 0.0	4.84 ± 0.0	4.63 ± 0.25	10.62 ± 0.02	10.55 ± 0.01	6.73 ± 0.03	$\textbf{20.77} \pm \textbf{0.08}$	$\textbf{108.96} \pm \textbf{0.06}$
ParetoFlow	4.2 ± 0.17	4.86 ± 0.01	-	10.61 ± 0.0	11.12 ± 0.02	6.55 ± 0.59	19.41 ± 0.92	107.1 ± 6.96
PGD-MOO + Data Pruning (Ours)	4.42 ± 0.04	4.83 ± 0.01	4.84 ± 0.0	10.64 ± 0.0	10.43 ± 0.04	5.99 ± 0.18	19.37 ± 0.15	103.04 ± 1.71
PGD-MOO (Ours)	4.46 ± 0.03	$\textbf{4.84} \pm \textbf{0.0}$	$\textbf{4.84} \pm \textbf{0.0}$	$\textbf{10.65} \pm \textbf{0.0}$	10.32 ± 0.1	6.13 ± 0.12	19.31 ± 0.46	105.02 ± 1.14

5.2 Results

Evaluation of Convergence. We provide detailed results of hypervolume for various baselines and our approach on the synthetic task (Tables 2 and 3). We find that our approach performs competitively with respect to baselines. Preference-guided diffusion performs on average better than ParetoFlow, another generative model-based approach using guidance. This shows the benefits of having a preference model as a classifier for guidance. Vizualization of the final sampled designs from our approach is provided in Appendix E.2. Overall, our method performs better than other baselines, which learn surrogate models and use evolutionary algorithms in the **synthetic** task setting (Fig. 3). In addition, we also find that our method performs competitively in the **RE** engineering suite (Tables 4 and 22) and the MO-NAS tasks (Table 1). In problems with higher number of objectives, we find that our approach is slightly worse compared to the baselines in terms of hypervolume. However, we note that our approach is much simpler to train in these settings, while still achieving diverse solutions (discussed further below).

Evaluation of Diversity. Average ranking in terms of performance of the Δ -spread metric for all algorithms (Table 5) shows that our approach gives more diverse solutions than all the other baselines including in the **RE** setting. These results highlight the importance of having a diversity constraint in the training procedure for the classifier through the data selection procedure (Appendix E.3).

Across experiments, we find that our approach has competitive performance in terms of hypervolume (convergence) while being better in terms of the Δ -spread metric (diversity) than the baselines.

5.3 Ablation Studies

We also study the impact of choice of two important aspects: the guidance-weight hyperaprameter w, and the role of diversity criteria in training the preference classifier.

Results for various choices of w for ZDT subtask are provided in Fig. 4a. With w=0 (no preference guidance), the results are lower, as expected. Increasing the guidance weight generally results in better hypervolume at the slight cost of diversity. This indicates that if diversity is more important in the resulting designs, extreme values of w are less preferable.

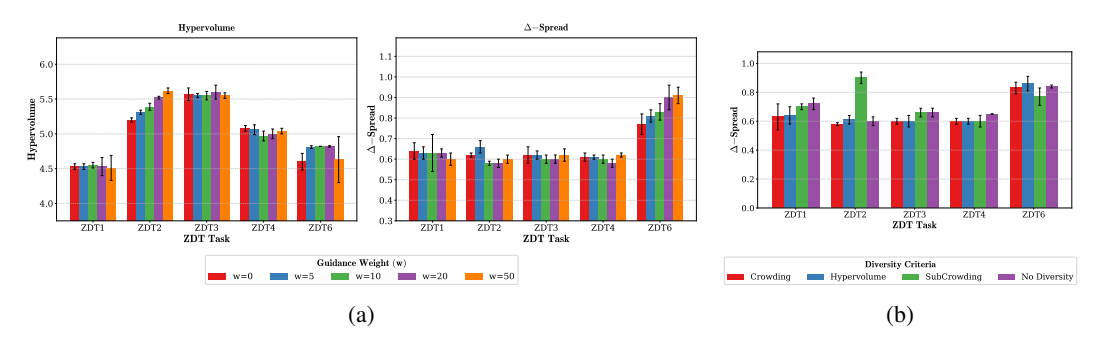


Figure 4: Ablation study of (a) different guidance weights w on both hypervolume and Δ -spread metrics (b) various diversity criteria (Crowding, SubCrowding, No Diversity and Hypervolume) on the Δ -spread metric. All evaluation done with ZDT subtask on 256 sampled designs across 5 random seeds.

We also perform ablation studies on the role of diversity criteria that is used to pick preference pairs for training the preference classifier. For an effective comparison, we also compare with hypervolume improvement, in addition to Crowding, SubCrowding and having no diversity criteria. In the hypervolume improvement diversity metric (indicated as just Hypervolume), we measure diversity of a point based on the change in hypervolume it brings when it is added to the sampled set of designs. Results for Δ -spread metric for the ZDT subtask is given in Fig. 4b. We find that incorporating diversity criteria for preference generally results in better diversity of the resulting solutions. In addition, Crowding and SubCrowding gives better diversity than using hypervolume improvement.

Table 5: Average ranking of the Δ -spread metric obtained by different algorithms on both synthetic and RE tasks. Detailed results are provided in Appendix E.

Method	Synthetic	RE
MultiHead-GradNorm	7.12	8.27
MultiHead-PcGrad	5.92	7.0
MultiHead	8.83	7.2
MultipleModels-COM	6.5	5.47
MultipleModels-ICT	6.5	5.87
MultipleModels-IOM	6.42	6.8
MultipleModels-RoMA	5.92	6.4
MultipleModels-TriMentoring	6.0	4.6
MultipleModels	9.25	7.53
ParetoFlow	10.0	9.0
PGD-MOO + Pruning (Ours)	2.67	4.0
PGD-MOO (Ours)	2.83	4.28

Detailed results for all tasks are provided in Appendix E.1.

6 Conclusion

In this work, we presented a novel classifier-guided diffusion approach for offline multi-objective optimization (MOO). Our method leverages a preference model that predicts Pareto dominance between pairs of inputs, incorporating diversity considerations to ensure that designs on the same Pareto front are well-distributed. Empirical results show that our technique performs competitively in terms of convergence to the true Pareto front, while also generating a diverse set of solutions.

Limitations. A key limitation of our current approach is that it relies solely on dominance information rather than the individual function values of the objectives. Consequently, it does not allow fine-grained control over trade-offs among different objectives, which can be important if a practitioner needs to emphasize or de-emphasize specific objective values.

Future Directions. One promising extension would be to integrate additional guidance signals, such as the actual function values, enabling a more preference-based form of MOO. This would allow users to explicitly prioritize certain objectives over others or specify desired performance ranges. Another avenue for future work is combining forward (surrogate-based) and inverse (generative) approaches, where candidates proposed by the generative model are iteratively refined using surrogate models.

Acknowledgements

This work was supported by a CIFAR Catalyst grant, the Helmholtz Foundation Model Initiative and the Helmholtz Association. The authors also acknowledge the Gauss Centre for Supercomputing e.V. (www.gauss-centre.eu) for funding this project by providing computing time on the GCS Supercomputer JUQUEEN [37] at Jülich Supercomputing Centre (JSC). BEE was funded in part by grants from the Parker Institute for Cancer Immunology (PICI), the Chan-Zuckerberg Institute (CZI), NIH NHGRI R01 HG012967, and NIH NHGRI R01 HG013736. BEE is a CIFAR Fellow in the Multiscale Human Program. Syrine Belakaria is supported by the Stanford Data Science fellowship.

References

- [1] Alaleh Ahmadianshalchi, Syrine Belakaria, and Janardhan Rao Doppa. Pareto front-diverse batch multi-objective bayesian optimization. In *Proceedings of the AAAI Conference on Artificial Intelligence*, volume 38, pages 10784–10794, 2024.
- [2] Charles Audet, Jean Bigeon, Dominique Cartier, Sébastien Le Digabel, and Ludovic Salomon. Performance indicators in multiobjective optimization. *European journal of operational research*, 292(2):397–422, 2021.
- [3] Maximilian Balandat, Brian Karrer, Daniel Jiang, Samuel Daulton, Ben Letham, Andrew G Wilson, and Eytan Bakshy. Botorch: A framework for efficient monte-carlo bayesian optimization. *Advances in neural information processing systems*, 33:21524–21538, 2020.
- [4] Syrine Belakaria, Aryan Deshwal, and Janardhan Rao Doppa. Output space entropy search framework for multi-objective bayesian optimization. *Journal of artificial intelligence research*, 72:667–715, 2021.
- [5] Ralph Allan Bradley and Milton E Terry. Rank analysis of incomplete block designs: I. the method of paired comparisons. *Biometrika*, 39(3/4):324–345, 1952.
- [6] David Brookes, Hahnbeom Park, and Jennifer Listgarten. Conditioning by adaptive sampling for robust design. In *International conference on machine learning*, pages 773–782. PMLR, 2019.
- [7] Yassine Chemingui, Aryan Deshwal, Trong Nghia Hoang, and Janardhan Rao Doppa. Offline model-based optimization via policy-guided gradient search. In *Proceedings of the AAAI Conference on Artificial Intelligence*, volume 38, pages 11230–11239, 2024.
- [8] Can Sam Chen, Christopher Beckham, Zixuan Liu, Xue Liu, and Christopher Pal. Robust guided diffusion for offline black-box optimization. *arXiv preprint arXiv:2410.00983*, 2024.
- [9] Can Sam Chen, Christopher Beckham, Zixuan Liu, Xue Steve Liu, and Chris Pal. Parallel-mentoring for offline model-based optimization. Advances in Neural Information Processing Systems, 36, 2024.
- [10] Zhao Chen, Vijay Badrinarayanan, Chen-Yu Lee, and Andrew Rabinovich. Gradnorm: Gradient normalization for adaptive loss balancing in deep multitask networks. In *International conference on machine learning*, pages 794–803. PMLR, 2018.
- [11] Samuel Daulton, Maximilian Balandat, and Eytan Bakshy. Differentiable expected hypervolume improvement for parallel multi-objective bayesian optimization. *Advances in Neural Information Processing Systems*, 33:9851–9864, 2020.
- [12] Kalyanmoy Deb, Amrit Pratap, Sameer Agarwal, and TAMT Meyarivan. A fast and elitist multiobjective genetic algorithm: Nsga-ii. *IEEE transactions on evolutionary computation*, 6 (2):182–197, 2002.
- [13] Prafulla Dhariwal and Alexander Nichol. Diffusion models beat gans on image synthesis. *Advances in neural information processing systems*, 34:8780–8794, 2021.
- [14] Xuanyi Dong and Yi Yang. Nas-bench-201: Extending the scope of reproducible neural architecture search. *arXiv preprint arXiv:2001.00326*, 2020.

- [15] Michael Emmerich and Jan-willem Klinkenberg. The computation of the expected improvement in dominated hypervolume of pareto front approximations. *Rapport technique, Leiden University*, 34:7–3, 2008.
- [16] Clara Fannjiang and Jennifer Listgarten. Autofocused oracles for model-based design. Advances in Neural Information Processing Systems, 33:12945–12956, 2020.
- [17] Jonathan Ho, Ajay Jain, and Pieter Abbeel. Denoising diffusion probabilistic models. *Advances in neural information processing systems*, 33:6840–6851, 2020.
- [18] Donald R Jones, Matthias Schonlau, and William J Welch. Efficient global optimization of expensive black-box functions. *Journal of Global optimization*, 13:455–492, 1998.
- [19] Minsu Kim, Jiayao Gu, Ye Yuan, Taeyoung Yun, Zixuan Liu, Yoshua Bengio, and Can Chen. Offline model-based optimization: Comprehensive review. arXiv preprint arXiv:2503.17286, 2025.
- [20] Diederik P Kingma. Adam: A method for stochastic optimization. arXiv preprint arXiv:1412.6980, 2014.
- [21] Joshua Knowles. Parego: A hybrid algorithm with on-line landscape approximation for expensive multiobjective optimization problems. *IEEE transactions on evolutionary computation*, 10 (1):50–66, 2006.
- [22] Mina Konakovic Lukovic, Yunsheng Tian, and Wojciech Matusik. Diversity-guided multiobjective bayesian optimization with batch evaluations. *Advances in Neural Information Processing Systems*, 33:17708–17720, 2020.
- [23] Siddarth Krishnamoorthy, Satvik Mehul Mashkaria, and Aditya Grover. Generative pretraining for black-box optimization. *arXiv preprint arXiv:2206.10786*, 2022.
- [24] Siddarth Krishnamoorthy, Satvik Mehul Mashkaria, and Aditya Grover. Diffusion models for black-box optimization. In *International Conference on Machine Learning*, pages 17842–17857. PMLR, 2023.
- [25] Aviral Kumar and Sergey Levine. Model inversion networks for model-based optimization. Advances in neural information processing systems, 33:5126–5137, 2020.
- [26] Jimmy Lei Ba, Jamie Ryan Kiros, and Geoffrey E Hinton. Layer normalization. *ArXiv e-prints*, pages arXiv–1607, 2016.
- [27] Chaojian Li, Zhongzhi Yu, Yonggan Fu, Yongan Zhang, Yang Zhao, Haoran You, Qixuan Yu, Yue Wang, and Yingyan Lin. Hw-nas-bench: Hardware-aware neural architecture search benchmark. *arXiv preprint arXiv:2103.10584*, 2021.
- [28] Yaron Lipman, Ricky TQ Chen, Heli Ben-Hamu, Maximilian Nickel, and Matt Le. Flow matching for generative modeling. arXiv preprint arXiv:2210.02747, 2022.
- [29] I Loshchilov. Decoupled weight decay regularization. arXiv preprint arXiv:1711.05101, 2017.
- [30] Zhichao Lu, Ran Cheng, Yaochu Jin, Kay Chen Tan, and Kalyanmoy Deb. Neural architecture search as multiobjective optimization benchmarks: Problem formulation and performance assessment. *IEEE transactions on evolutionary computation*, 28(2):323–337, 2023.
- [31] Han Qi, Yi Su, Aviral Kumar, and Sergey Levine. Data-driven offline decision-making via invariant representation learning. *Advances in Neural Information Processing Systems*, 35: 13226–13237, 2022.
- [32] Rafael Rafailov, Archit Sharma, Eric Mitchell, Christopher D Manning, Stefano Ermon, and Chelsea Finn. Direct preference optimization: Your language model is secretly a reward model. *Advances in neural information processing systems*, 36:53728–53741, 2023.
- [33] Bobak Shahriari, Kevin Swersky, Ziyu Wang, Ryan P Adams, and Nando De Freitas. Taking the human out of the loop: A review of bayesian optimization. *Proceedings of the IEEE*, 104 (1):148–175, 2015.

- [34] Jascha Sohl-Dickstein, Eric Weiss, Niru Maheswaranathan, and Surya Ganguli. Deep unsupervised learning using nonequilibrium thermodynamics. In *International conference on machine learning*, pages 2256–2265. PMLR, 2015.
- [35] Yang Song, Jascha Sohl-Dickstein, Diederik P Kingma, Abhishek Kumar, Stefano Ermon, and Ben Poole. Score-based generative modeling through stochastic differential equations. arXiv preprint arXiv:2011.13456, 2020.
- [36] Samuel Stanton, Wesley Maddox, Nate Gruver, Phillip Maffettone, Emily Delaney, Peyton Greenside, and Andrew Gordon Wilson. Accelerating bayesian optimization for biological sequence design with denoising autoencoders. In *International Conference on Machine Learning*, pages 20459–20478. PMLR, 2022.
- [37] Michael Stephan and Jutta Docter. Juqueen: Ibm blue gene/q® supercomputer system at the jülich supercomputing centre. *Journal of large-scale research facilities JLSRF*, 1:A1–A1, 2015.
- [38] Jonathan M Stokes, Kevin Yang, Kyle Swanson, Wengong Jin, Andres Cubillos-Ruiz, Nina M Donghia, Craig R MacNair, Shawn French, Lindsey A Carfrae, Zohar Bloom-Ackermann, et al. A deep learning approach to antibiotic discovery. *Cell*, 180(4):688–702, 2020.
- [39] Kyle Swanson, Gary Liu, Denise B Catacutan, Autumn Arnold, James Zou, and Jonathan M Stokes. Generative ai for designing and validating easily synthesizable and structurally novel antibiotics. *Nature Machine Intelligence*, 6(3):338–353, 2024.
- [40] Ryoji Tanabe and Hisao Ishibuchi. An easy-to-use real-world multi-objective optimization problem suite. *Applied Soft Computing*, 89:106078, 2020.
- [41] Brandon Trabucco, Aviral Kumar, Xinyang Geng, and Sergey Levine. Conservative objective models for effective offline model-based optimization. In *International Conference on Machine Learning*, pages 10358–10368. PMLR, 2021.
- [42] Brandon Trabucco, Xinyang Geng, Aviral Kumar, and Sergey Levine. Design-bench: Benchmarks for data-driven offline model-based optimization. In *International Conference on Machine Learning*, pages 21658–21676. PMLR, 2022.
- [43] A Vaswani. Attention is all you need. Advances in Neural Information Processing Systems, 2017.
- [44] Christopher KI Williams and Carl Edward Rasmussen. *Gaussian processes for machine learning*, volume 2. MIT press Cambridge, MA, 2006.
- [45] Ke Xue, Rong-Xi Tan, Xiaobin Huang, and Chao Qian. Offline multi-objective optimization. *arXiv preprint arXiv:2406.03722*, 2024.
- [46] Sihyun Yu, Sungsoo Ahn, Le Song, and Jinwoo Shin. Roma: Robust model adaptation for offline model-based optimization. Advances in Neural Information Processing Systems, 34: 4619–4631, 2021.
- [47] Tianhe Yu, Saurabh Kumar, Abhishek Gupta, Sergey Levine, Karol Hausman, and Chelsea Finn. Gradient surgery for multi-task learning. *Advances in Neural Information Processing Systems*, 33:5824–5836, 2020.
- [48] Ye Yuan, Can Chen, Christopher Pal, and Xue Liu. Paretoflow: Guided flows in multi-objective optimization. *arXiv preprint arXiv:2412.03718*, 2024.
- [49] Ye Yuan, Can Sam Chen, Zixuan Liu, Willie Neiswanger, and Xue Steve Liu. Importance-aware co-teaching for offline model-based optimization. *Advances in Neural Information Processing Systems*, 36, 2024.
- [50] Yu Zhang and Qiang Yang. A survey on multi-task learning. *IEEE transactions on knowledge and data engineering*, 34(12):5586–5609, 2021.

- [51] Aimin Zhou, Yaochu Jin, Oingfu Zhang, Bernhard Sendhoff, and Edward Tsang. Combining model-based and genetics-based offspring generation for multi-objective optimization using a convergence criterion. In 2006 IEEE international conference on evolutionary computation, pages 892-899. IEEE, 2006.
- [52] Eckart Zitzler and Lothar Thiele. Multiobjective optimization using evolutionary algorithms—a comparative case study. In International conference on parallel problem solving from nature, pages 292-301. Springer, 1998.
- [53] Eckart Zitzler, Kalyanmoy Deb, and Lothar Thiele. Comparison of multiobjective evolutionary algorithms: Empirical results. Evolutionary computation, 8(2):173-195, 2000.

NeurIPS Paper Checklist

1. Claims

Question: Do the main claims made in the abstract and introduction accurately reflect the paper's contributions and scope?

Answer: [Yes]

Justification: The paper's contributions are using a preference based guidance for diffusion models in an offline MOO setting. This is laid out in the abstract.

2. Limitations

Question: Does the paper discuss the limitations of the work performed by the authors?

Answer: [Yes]

Justification: Limitations are laid out in §6.

3. Theory assumptions and proofs

Question: For each theoretical result, does the paper provide the full set of assumptions and a complete (and correct) proof?

Answer: [No]

Justification: The paper does not provide any formal theoretical results.

4. Experimental result reproducibility

Question: Does the paper fully disclose all the information needed to reproduce the main experimental results of the paper to the extent that it affects the main claims and/or conclusions of the paper (regardless of whether the code and data are provided or not)?

Answer: [Yes]

Justification: The required details for reproducibility is provided in §5.

5. Open access to data and code

Ouestion: Does the paper provide open access to the data and code, with sufficient instructions to faithfully reproduce the main experimental results, as described in supplemental material?

Answer: [Yes]

Justification: The reproducible code is included as part of the submission in the supplementary material.

6. Experimental setting/details

Question: Does the paper specify all the training and test details (e.g., data splits, hyperparameters, how they were chosen, type of optimizer, etc.) necessary to understand the results?

Answer: [Yes]

Justification: The training and testing details are laid out in §5.

7. Experiment statistical significance

Question: Does the paper report error bars suitably and correctly defined or other appropriate information about the statistical significance of the experiments?

Answer: [Yes]

Justification: All experiments are conducted with multiple seeds and confidence intervals are provided.

8. Experiments compute resources

Question: For each experiment, does the paper provide sufficient information on the computer resources (type of compute workers, memory, time of execution) needed to reproduce the experiments?

Answer: [Yes]

Justification: Details regarding computational resources needed for experiments is provided in Appendix C.

9. Code of ethics

Question: Does the research conducted in the paper conform, in every respect, with the NeurIPS Code of Ethics https://neurips.cc/public/EthicsGuidelines?

Answer: [Yes]

Justification: The authors have reviewed the NeurIPS code of ethics and the research conducted in the paper conforms to this code.

10. Broader impacts

Question: Does the paper discuss both potential positive societal impacts and negative societal impacts of the work performed?

Answer: [Yes]

Justification: Broader impact statement is provided in Appendix D.

11. Safeguards

Question: Does the paper describe safeguards that have been put in place for responsible release of data or models that have a high risk for misuse (e.g., pretrained language models, image generators, or scraped datasets)?

Answer: [NA]

Justification: The paper does not deal with an algorithm or model that have potential for high risk of misuse.

12. Licenses for existing assets

Question: Are the creators or original owners of assets (e.g., code, data, models), used in the paper, properly credited and are the license and terms of use explicitly mentioned and properly respected?

Answer: [NA]

Justification: The licenses for the code and which this paper relies on is from [45], whose code has been released on Github with an unknown license.

13. New assets

Question: Are new assets introduced in the paper well documented and is the documentation provided alongside the assets?

Answer: [NA]

Justification: The paper does not release new assets.

14. Crowdsourcing and research with human subjects

Question: For crowdsourcing experiments and research with human subjects, does the paper include the full text of instructions given to participants and screenshots, if applicable, as well as details about compensation (if any)?

Answer: [NA]

Justification: The paper does not involve crowdsourcing nor research with human subjects.

15. Institutional review board (IRB) approvals or equivalent for research with human subjects

Question: Does the paper describe potential risks incurred by study participants, whether such risks were disclosed to the subjects, and whether Institutional Review Board (IRB) approvals (or an equivalent approval/review based on the requirements of your country or institution) were obtained?

Answer: [NA]

Justification: The paper does not involve crowdsourcing nor research with human subjects.

16. Declaration of LLM usage

Question: Does the paper describe the usage of LLMs if it is an important, original, or non-standard component of the core methods in this research? Note that if the LLM is used only for writing, editing, or formatting purposes and does not impact the core methodology, scientific rigorousness, or originality of the research, declaration is not required.

Answer: [NA]

Justification: The core method development in this research does not involve LLMs.

Appendix: Preference-Guided Diffusion for Multi-Objective Offline Optimization

A Experimental Setting

A.1 Metrics

We provide computational details regarding the metrics used in the work - hypervolume and Δ -spread.

• Hypervolume: Hypervolume is a common metric which is used in Multi-Objective Optimization to measure the quality of the solutions. It does not require access to the Pareto-Front. It instead relies on a reference point, which is any point in the input space that is worse than all points in the solution set across every objective. Given this reference point x_{ref} , hypervolume is computed as the area enclosed by hyperrectangle from every point in the solution set S to x_{ref} :

$$HV(S) := \int \bigcup_{\boldsymbol{x} \in S} [\boldsymbol{x}_1, \boldsymbol{x}_{ref_1}] \times [\boldsymbol{x}_2, \boldsymbol{x}_{ref_2}] \times \cdots \times [\boldsymbol{x}_m, \boldsymbol{x}_{ref_m}] \ d\lambda \tag{8}$$

where λ is the Lebesgue measure and $[\cdot,\cdot]$ corresponds to a hyperrectangle between the two points. While relatively easier for 2 or 3 objective problems, computing hypervolume is more involved for solutions with higher number of objectives.

• Δ -Spread: Δ -Spread [12, 51] measures the uniformity of solutions which belong to the same front. In this work, we take into account the extreme points of the predicted front to calculate the Δ -spread of a solution set S as follows:

$$\Delta(S) := \frac{\sum_{i=1}^{m} \min_{y} ||y^{i,*} - y|| + \sum_{k=1}^{|S|-1} \left[d^{c}(y^{k}, S/\{y^{k}\}) - \hat{d}^{c} \right]}{\sum_{i=1}^{m} \min_{y} ||y^{i,*} - y|| + (|S| - 1)\hat{d}^{c}}$$
(9)

where $\min_y ||y^{i,*} - y||$ is the distance between the extreme points of the set S and the corresponding extreme points in the Pareto front. If the Pareto front is not known, this quantity is evaluated to be zero. $d^c(y^k, S/\{y^k\})$ corresponds to the distance between consecutive points of set S, sorted according to objective values of one of the objectives, and \hat{d}^c is the mean of d^c across all elements of set S.

B Dataset Details

We provide further details of the datasets used in our experiments for both Synthetic and RE set of tasks in Tables 6 and 7. All the datasets are directly taken from [45] as well as the evaluation of hypervolume computation and the needed reference points.

Table 6: Dataset information and reference point for hypervolume computation Synthetic set of tasks.

Name	d	m	Pareto Front Shape	Reference Point
DTLZ1	7	3	Linear	(558.21, 552.30, 568.36)
DTLZ2	10	3	Concave	(2.77, 2.78, 2.93)
DTLZ3	10	3	Concave	(1703.72, 1605.54, 1670.48)
DTLZ4	10	3	Concave	(3.03, 2.83, 2.78)
DTLZ5	10	3	Concave (2d)	(2.65, 2.61, 2.70)
DTLZ6	10	3	Concave (2d)	(9.80, 9.78, 9.78)
DTLZ7	10	3	Disconnected	(1.10, 1.10, 33.43)
ZDT1	30	2	Convex	(1.10, 8.58)
ZDT2	30	2	Concave	(1.10, 9.59)
ZDT3	30	2	Disconnected	(1.10, 8.74)
ZDT4	10	2	Convex	(1.10, 300.42)
ZDT6	10	2	Concave	(1.07, 10.27)

Table 7: Dataset information and reference point for hypervolume computation for **RE** set of tasks.

Name	d	m	Pareto Front Shape	Reference Point
RE21 (Four bar truss design)	4	2	Convex	(3144.44, 0.05)
RE22 (Reinforced concrete beam design)	3	2	Mixed	(829.08, 2407217.25)
RE23 (Pressure vessel design)	4	2	Mixed, Disconnected	(713710.88, 1288669.78)
RE24 (Hatch cover design)	2	2	Convex	(5997.83, 43.67)
RE25 (Coil compression spring design)	3	2	Mixed, Disconnected	(124.79, 10038735.00)
RE31 (Two bar truss design)	3	3	Unknown	(808.85, 6893375.82, 6793450.00)
RE32 (Welded beam design)	4	3	Unknown	(290.66, 16552.46, 388265024.00)
RE33 (Disc brake design)	4	3	Unknown	(8.01, 8.84, 2343.30)
RE34 (Vehicle crashworthiness design)	5	3	Unknown	(1702.52, 11.68, 0.26)
RE35 (Speed reducer design)	7	3	Unknown	(7050.79, 1696.67, 397.83)
RE36 (Gear train design)	4	3	Concave, Disconnected	(10.21, 60.00, 0.97)
RE37 (Rocket injector design)	4	3	Unknown	(0.99, 0.96, 0.99)
RE41 (Car side impact design)	7	4	Unknown	(42.65, 4.43, 13.08, 13.45)
RE42 (Conceptual marine design)	6	4	Unknown	(-26.39, 19904.90, 28546.79, 14.98)
RE61 (Water resource planning)	3	6	Unknown	(83060.03, 1350.00, 2853469.06,
				16027067.60, 357719.74, 99660.36)

Table 8: Dataset information and reference point for MO-NAS set of tasks.

Name	Search space	d	m	Reference Point
C-10/MOP1	NAS-Bench-101	26	2	$(3.49 \times 10^{-1}, 3.14 \times 10^7)$
C-10/MOP2	NAS-Bench-101	26	3	$(9.05 \times 10^{-1}, 3.05 \times 10^{7}, 8.97 \times 10^{0})$
C-10/MOP3	NATS	5	3	$(2.31 \times 10^{1}, 7.14 \times 10^{-1}, 2.74 \times 10^{2})$
C-10/MOP4	NATS	5	4	$(2.31 \times 10^{1}, 7.14 \times 10^{-1}, 2.74 \times 10^{2}, 2.12 \times 10^{-2})$
C-10/MOP5	NAS-Bench-201	6	5	$(9.03 \times 10^{1}, 1.53 \times 10^{0}, 2.20 \times 10^{2}, 1.17 \times 10^{1}, 4.88 \times 10^{1})$
C-10/MOP6	NAS-Bench-201	6	6	$(9.03 \times 10^{1}, 1.53 \times 10^{0}, 2.20 \times 10^{2}, 1.05 \times 10^{1}, 2.23 \times 10^{0}, 2.76 \times 10^{1})$
C-10/MOP7	NAS-Bench-201	6	8	$(9.03 \times 10^1, 1.53 \times 10^0, 2.20 \times 10^2, 1.17 \times 10^1,$
				$4.88 \times 10^{1}, 1.05 \times 10^{1}, 2.23 \times 10^{0}, 2.76 \times 10^{1})$
C-10/MOP8	DARTS	32	2	$(2.61 \times 10^{-1}, 1.55 \times 10^{6})$
C-10/MOP9	DARTS	32	3	$(4.85 \times 10^{-2}, 3.92 \times 10^5)$
IN-1K/MOP1	ResNet50	25	2	$(2.81 \times 10^{-1}, 3.95 \times 10^7)$
IN-1K/MOP2	ResNet50	25	2	$(2.80 \times 10^{-1}, 1.15 \times 10^{10})$
IN-1K/MOP3	ResNet50	25	3	$(2.81 \times 10^{-1}, 3.87 \times 10^{7}, 1.26 \times 10^{10})$
IN-1K/MOP4	Transformer	34	2	$(1.83 \times 10^1, 7.25 \times 10^7)$
IN-1K/MOP5	Transformer	34	3	$(1.83 \times 10^1, 1.49 \times 10^{10})$
IN-1K/MOP6	Transformer	34	3	$(1.83 \times 10^1, 7.10 \times 10^7, 1.48 \times 10^{10})$
IN-1K/MOP7	MNV3	21	2	$(2.64 \times 10^{-1}, 9.98 \times 10^{6})$
IN-1K/MOP8	MNV3	21	3	$(2.65 \times 10^{-1}, 1.00 \times 10^{7}, 1.34 \times 10^{9})$
IN-1K/MOP9	MNV3	21	4	$(2.65 \times 10^{-1}, 1.03 \times 10^{7}, 1.31 \times 10^{9}, 6.30 \times 10^{1})$

C Computational Resources

All the experiments are run on an NVIDIA A100 GPU. Our proposed approach takes on average of 1300 seconds for a 2 objective task of 30 dimensions. Approaches like MultipleModels' walltime is directly proportional to the number of objectives. Consequently, Paretoflow [48], which relies on MultipleModels also scales poorly wrt number of objectives. Overall, our approach takes roughly 56 GPU hours to train and test on all the datasets for 5 seeds. A representative runtime of our approach as well as the baselines is given in Table 9.

D Broader Impact Statement

This paper addresses the problem of offline optimization with multiple objectives. Advances in the problem being addressed are impactful for discovering new drugs for curing diseases, discovering new materials with certain physical properties, to name a few. The authors do not forsee any negative societal impacts of this work beyond what might be enabled due to general advancements in machine learning.

Table 9: Runtime (in seconds, for training) of different approaches on two representative tasks. Both tasks have 60k samples in total. The runtime of PGD mainly depends on the dimensionality of the problem (for RE 61 it is 3 and ZDT1 is 30) while for approaches like MultiHead and ParetoFlow it is proportional to the number of objectives (for RE 61 it is 6 and for ZDT1 it is 2), since they require training a surrogate model for each objective. We expect these runtimes to be the same if the dimensionality (or correspondingly the number of objectives) for other tasks are the same. Sampling times for all these approaches are fairly fast (at most 30 sec for 256 samples).

Method	ZDT1	RE61
MultiHead	450	470
MultipleModels	920	2820
ParetoFlow	1200	3100
PGD-MOO (Ours)	1300	930

E Additional Results

E.1 Ablation Study Full Results

In addition to the main results, we perform evaluation of the impact of guidance weight w on the resulting designs. Tables 10, 12 and 14 presents results of hypervolume evaluated on 256 sampled designs. Tables 11, 13 and 15 presents the corresponding diversity evaluation with Δ -spread metric.

In addition to the above evaluation, we also evaluate the impact of the incporated diversity criteria for selecting the preference pairs for training the classifer. In addition to *Crowding* and *SubCrowding*, we also consider not incorporating any diversity (mentioned as *No diversity*), as well as computing the improvement in hypervolume due to specific design in the sampled designs (mentioned as just *Hypervolume*). Hypervolume improvement due to a specific sample can be computed as the difference between hypervolume due to the entire set and the hypervolume due to the entire set except for this specific sample.

Results for different evaluation criteria are provided in Tables 16, 18 and 20 for hypervolume, as well as in Tables 17, 19 and 21 for diversity.

Table 10: Hypervolume results with 256 sampled designs of different guidance weights w for DTLZ subtasks (part of **synthetic** task).

Guidance Weight (w)	DTLZ1	DTLZ2	DTLZ3	DTLZ4	DTLZ5	DTLZ6	DTLZ7
w = 0	10.64±0.00	10.53 ± 0.02	10.61 ± 0.02	10.66 ± 0.01	10.07 ± 0.02	10.15 ± 0.05	9.48 ± 0.14
w = 5	10.65 ± 0.00	10.54 ± 0.02	10.63 ± 0.00	10.64 ± 0.01	10.08 ± 0.01	10.17 ± 0.02	9.64 ± 0.14
w = 10	10.65 ± 0.00	10.56 ± 0.00	10.63 ± 0.00	10.65 ± 0.01	10.05 ± 0.01	10.17 ± 0.04	9.76 ± 0.14
w = 20	10.64 ± 0.00	10.55 ± 0.01	10.62 ± 0.01	10.64 ± 0.01	10.09 ± 0.02	10.16 ± 0.04	9.81 ± 0.23
w = 50	10.62 ± 0.01	10.55 ± 0.01	10.63 ± 0.00	10.63 ± 0.01	10.09 ± 0.02	10.16 ± 0.09	$9.80 {\pm} 0.36$

Table 11: Diversity evaluation results with 256 sampled designs of different guidance weights w for DTLZ subtasks (part of **synthetic** task).

Guidance Weight (w)	DTLZ1	DTLZ2	DTLZ3	DTLZ4	DTLZ5	DTLZ6	DTLZ7
w = 0	0.54 ± 0.02	0.54 ± 0.02	0.48 ± 0.01	1.66 ± 0.03	0.50 ± 0.02	0.64 ± 0.01	0.52 ± 0.02
w = 5	0.59 ± 0.04	0.54 ± 0.03	0.48 ± 0.03	1.62 ± 0.04	0.52 ± 0.04	0.62 ± 0.02	0.65 ± 0.04
w = 10	0.61 ± 0.04	0.56 ± 0.02	0.47 ± 0.02	1.62 ± 0.03	0.54 ± 0.02	0.62 ± 0.02	0.70 ± 0.05
w = 20	0.61 ± 0.05	0.54 ± 0.03	0.47 ± 0.01	1.53 ± 0.02	0.50 ± 0.03	0.60 ± 0.03	0.73 ± 0.07
w = 50	0.60 ± 0.01	$0.56 {\pm} 0.02$	0.49 ± 0.03	1.49 ± 0.05	0.53 ± 0.03	0.60 ± 0.02	0.66 ± 0.06

Table 12: Hypervolume results with 256 sampled designs of different guidance weights w for ZDT subtasks (part of **synthetic** task).

Guidance Weight (w)	ZDT1	ZDT2	ZDT3	ZDT4	ZDT6
w = 0	4.53±0.04	5.20 ± 0.03	5.57 ± 0.09	5.08 ± 0.04	4.60 ± 0.12
w = 5	4.53 ± 0.04	5.31 ± 0.03	5.55 ± 0.03	5.06 ± 0.07	4.81 ± 0.02
w = 10	4.55 ± 0.04	5.39 ± 0.05	5.55 ± 0.06	4.97 ± 0.07	4.82 ± 0.00
w = 20	4.53 ± 0.13	5.52 ± 0.02	5.60 ± 0.10	5.00 ± 0.07	4.82 ± 0.01
w = 50	4.51 ± 0.18	5.62 ± 0.04	5.55 ± 0.04	5.04 ± 0.04	4.63 ± 0.33

Table 13: Diversity evaluation results with 256 sampled designs of different guidance weights w in ZDT subtasks (part of **synthetic** task).

Guidance Weight (w)	ZDT1	ZDT2	ZDT3	ZDT4	ZDT6
w = 0	0.64 ± 0.04	0.62 ± 0.01	0.62 ± 0.04	0.61 ± 0.02	0.77 ± 0.05
w = 5	0.63 ± 0.03	0.66 ± 0.03	0.62 ± 0.02	0.61 ± 0.01	0.81 ± 0.03
w = 10	0.63 ± 0.09	0.58 ± 0.01	0.60 ± 0.02	0.60 ± 0.02	0.83 ± 0.04
w = 20	0.63 ± 0.02	0.58 ± 0.02	0.60 ± 0.02	0.58 ± 0.02	0.90 ± 0.06
w = 50	0.60 ± 0.03	0.60 ± 0.02	0.62 ± 0.03	0.62 ± 0.01	0.91 ± 0.04

Table 14: Hypervolume results with 256 sampled designs of different guidance weights w for various **RE** tasks.

Guidance Weight (w) RE21		RE24	RE25	RE35	RE41
w = 0	4.38±0.07	4.84 ± 0.00	$4.84{\pm}0.00$	10.42 ± 0.06	18.98 ± 0.25
w = 5	4.43 ± 0.05	4.84 ± 0.00	4.84 ± 0.00	10.37 ± 0.06	19.00 ± 0.26
w = 10	4.46 ± 0.04	4.83 ± 0.00	4.84 ± 0.00	10.27 ± 0.11	19.17 ± 0.30
w = 20	4.45 ± 0.05	4.84 ± 0.00	$4.84{\pm}0.00$	10.16 ± 0.15	18.40 ± 0.84
w = 50	4.44 ± 0.05	4.83 ± 0.00	4.84 ± 0.00	$9.55{\pm}0.54$	17.67 ± 0.96

Table 15: Diversity evaluation results with 256 sampled designs of different guidance weights w for various \mathbf{RE} tasks.

Guidance Weight (w)	RE21	RE24	RE25	RE35	RE41
w = 0	0.60 ± 0.03	1.15 ± 0.07	1.05 ± 0.05	0.70 ± 0.03	0.42 ± 0.02
w = 5	0.61 ± 0.04	1.20 ± 0.09	1.08 ± 0.05	0.81 ± 0.12	0.45 ± 0.02
w = 10	0.61 ± 0.02	1.20 ± 0.05	1.19 ± 0.08	1.00 ± 0.12	0.47 ± 0.04
w = 20	0.61 ± 0.03	1.18 ± 0.03	1.21 ± 0.06	0.83 ± 0.11	0.49 ± 0.04
w = 50	0.63 ± 0.02	1.17 ± 0.08	1.21 ± 0.06	$0.82 {\pm} 0.09$	0.62 ± 0.19

Table 16: Hypervolume results with 256 sampled designs when specific diversity criterion is used for training the preference classifier. Results evaluated with w=10 on DTLZ subtasks (part of **synthetic** tasks).

Diversity Criteria	DTLZ1	DTLZ2	DTLZ3	DTLZ4	DTLZ5	DTLZ6	DTLZ7
Crowding	10.65±0.00	10.56 ± 0.00	10.63 ± 0.00	10.65 ± 0.01	10.05 ± 0.01	10.17 ± 0.04	9.76±0.14
Hypervolume	10.64 ± 0.00	10.55 ± 0.01	10.63 ± 0.00	10.64 ± 0.00	10.06 ± 0.02	10.13 ± 0.01	9.72 ± 0.09
SubCrowding	10.64 ± 0.00	10.56 ± 0.01	10.62 ± 0.01	10.65 ± 0.02	10.08 ± 0.01	10.10 ± 0.07	9.49 ± 0.05
No diversity	10.64 ± 0.00	10.56 ± 0.00	10.63 ± 0.00	10.64 ± 0.01	10.06 ± 0.00	10.13 ± 0.00	9.66 ± 0.00

E.2 Visualization of the Sampled Designs

We provide visualization of the sampled designs from our model on 2-objective problems in Fig. 5.

Table 17: Diversity evaluation results with 256 sampled designs when specific diversity criterion is used for training the preference classifier. Results evaluated with w=10 on DTLZ subtasks (part of **synthetic** tasks).

Diversity Criteria	DTLZ1	DTLZ2	DTLZ3	DTLZ4	DTLZ5	DTLZ6	DTLZ7
Crowding	0.61 ± 0.04	0.56 ± 0.02	$0.47 {\pm} 0.02$	1.62 ± 0.03	$0.54 {\pm} 0.02$	$0.62 {\pm} 0.02$	0.70 ± 0.05
Hypervolume	0.58 ± 0.00	0.54 ± 0.03	0.49 ± 0.01	1.63 ± 0.04	0.53 ± 0.02	0.63 ± 0.02	0.76 ± 0.07
SubCrowding	0.55 ± 0.03	0.54 ± 0.02	0.48 ± 0.03	1.68 ± 0.04	0.51 ± 0.02	0.65 ± 0.02	0.58 ± 0.02
No diversity	0.58 ± 0.00	0.55 ± 0.00	0.48 ± 0.00	1.56 ± 0.03	0.53 ± 0.00	0.63 ± 0.00	0.68 ± 0.00

Table 18: Hypervolume results with 256 sampled designs when specific diversity criterion is used for training the preference classifier. Results evaluated with w=10 on ZDT subtasks (part of **synthetic** tasks).

Diversity Criteria	ZDT1	ZDT2	ZDT3	ZDT4	ZDT6
Crowding	4.55±0.04	5.39 ± 0.05	5.55 ± 0.06	4.97 ± 0.07	4.82±0.00
Hypervolume	4.49 ± 0.12	5.40 ± 0.05	5.59 ± 0.09	5.01 ± 0.11	4.82 ± 0.01
SubCrowding	4.54 ± 0.07	5.24 ± 0.04	5.60 ± 0.03	5.08 ± 0.08	4.59 ± 0.07
No diversity	4.59 ± 0.08	5.46 ± 0.03	5.58 ± 0.00	5.21 ± 0.00	4.74 ± 0.00

Table 19: Diversity evaluation results with 256 sampled designs when specific diversity criterion is used for training the preference classifier. Results evaluated with w=10 on ZDT subtasks (part of **synthetic** tasks).

Diversity Criteria	ZDT1	ZDT2	ZDT3	ZDT4	ZDT6
Crowding	0.63 ± 0.09	0.58 ± 0.01	0.60 ± 0.02	0.60 ± 0.02	0.83 ± 0.04
Hypervolume	0.64 ± 0.06	0.61 ± 0.03	0.60 ± 0.04	0.60 ± 0.02	$0.86{\pm}0.05$
SubCrowding	0.70 ± 0.02	0.90 ± 0.04	0.66 ± 0.03	0.60 ± 0.04	0.77 ± 0.06
No diversity	0.72 ± 0.04	0.60 ± 0.03	0.66 ± 0.03	0.65 ± 0.00	$0.84{\pm}0.01$

Table 20: Hypervolume results with 256 sampled designs when specific diversity criterion is used for training the preference classifier. Results evaluated with w=10 on ${\bf RE}$ tasks.

Diversity Criteria	RE21	RE24	RE25	RE35	RE41
Crowding	4.46 ± 0.04	4.83 ± 0.00	$4.84{\pm}0.00$	10.27 ± 0.11	19.17 ± 0.30
Hypervolume	4.41 ± 0.03	4.83 ± 0.00	4.84 ± 0.00	10.36 ± 0.04	19.09 ± 0.00
SubCrowding	4.39 ± 0.05	4.83 ± 0.00	4.84 ± 0.00	10.41 ± 0.05	19.02 ± 0.18
No diversity	4.42 ± 0.00	4.83 ± 0.00	$4.84{\pm}0.00$	10.35 ± 0.00	19.09 ± 0.00

Table 21: Diversity evaluation results with 256 sampled designs when specific diversity criterion is used for training the preference classifier. Results evaluated with w=10 on **RE** tasks.

Diversity Criteria	RE21	RE24	RE25	RE35	RE41
Crowding	0.61 ± 0.02	1.20 ± 0.05	1.19 ± 0.08	1.00 ± 0.12	0.47 ± 0.04
Hypervolume	0.62 ± 0.02	1.16 ± 0.09	1.14 ± 0.09	0.99 ± 0.08	0.47 ± 0.03
SubCrowding	0.60 ± 0.01	1.17 ± 0.05	1.12 ± 0.06	0.70 ± 0.03	0.43 ± 0.02
No diversity	0.62 ± 0.01	1.16 ± 0.06	1.39 ± 0.06	0.90 ± 0.02	0.50 ± 0.04

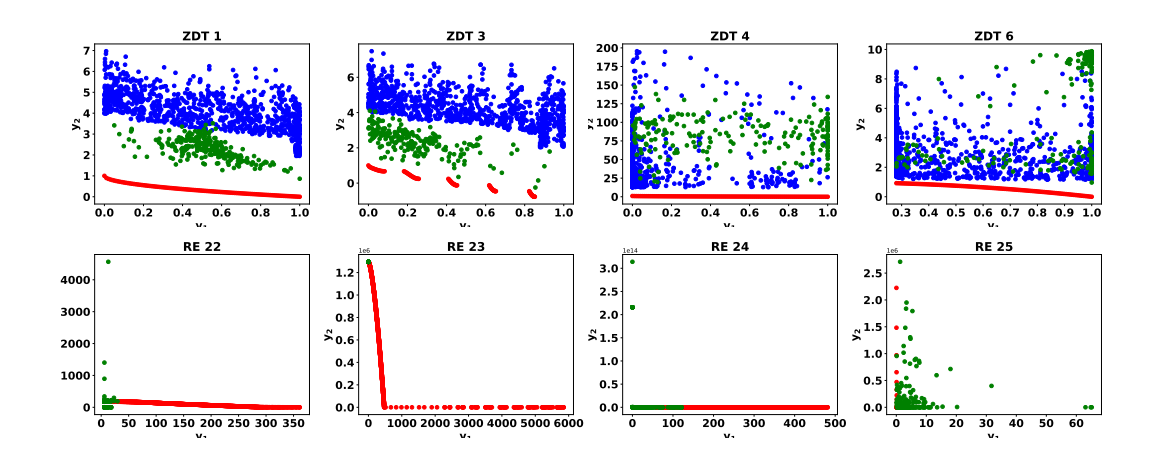


Figure 5: Plot of the samples from diffusion model (in green) on different 2-objective tasks. Top row shows results for synthetic set of benchmarks, while the bottom row shows results for RE engineering suite. Blue dots correspond to training data and red dot corresponds to the true Pareto front. The blue dots are omitted for the bottom row for clarity. Results for ZDT2 is available in Fig. 3.

Table 22: Evaluation of hypervolume with 256 sampled designs on subsets of the **RE** task. Results are averaged over 5 different random seeds.

Method	RE21	RE22	RE23	RE24	RE25	RE31	RE32	RE33
D(best)	4.1	4.78	4.75	4.6	4.79	10.6	10.56	10.56
MultiHead-GradNorm	4.28 ± 0.39	4.7 ± 0.44	3.77 ± 1.12	3.65 ± 0.82	4.52 ± 0.5	10.6 ± 0.1	10.54 ± 0.15	10.03 ± 1.5
MultiHead-PcGrad	4.59 ± 0.01	4.73 ± 0.36	4.84 ± 0.0	4.15 ± 0.66	4.78 ± 0.14	10.64 ± 0.01	10.63 ± 0.01	10.59 ± 0.03
MultiHead	4.6 ± 0.0	4.84 ± 0.0	4.84 ± 0.01	4.73 ± 0.2	4.74 ± 0.2	10.65 ± 0.0	10.6 ± 0.05	10.62 ± 0.0
MultipleModels-COM	4.38 ± 0.09	4.84 ± 0.0	4.84 ± 0.0	4.73 ± 0.2	4.83 ± 0.01	10.64 ± 0.01	10.64 ± 0.01	10.61 ± 0.0
MultipleModels-ICT	4.6 ± 0.0	4.84 ± 0.0	4.45 ± 0.02	4.83 ± 0.01	4.84 ± 0.0	10.65 ± 0.0	10.64 ± 0.0	10.62 ± 0.0
MultipleModels-IOM	4.58 ± 0.02	4.84 ± 0.0	4.83 ± 0.01	4.72 ± 0.11	4.83 ± 0.01	10.65 ± 0.0	10.65 ± 0.0	10.62 ± 0.0
MultipleModels-RoMA	4.57 ± 0.0	4.61 ± 0.51	4.83 ± 0.01	3.96 ± 1.2	4.83 ± 0.01	10.64 ± 0.01	10.64 ± 0.0	10.58 ± 0.03
MultipleModels-TriMentoring	4.6 ± 0.0	4.84 ± 0.0	4.84 ± 0.0	4.84 ± 0.0	4.84 ± 0.0	10.65 ± 0.0	10.62 ± 0.01	10.6 ± 0.01
MultipleModels	4.6 ± 0.0	4.84 ± 0.0	4.84 ± 0.0	4.83 ± 0.01	4.63 ± 0.25	10.65 ± 0.0	10.62 ± 0.02	10.62 ± 0.0
ParetoFlow	4.2 ± 0.17	4.86 ± 0.01	-	-	-	10.66 ± 0.12	10.61 ± 0.0	10.75 ± 0.2
PGD-MOO + Data Pruning (Ours)	4.42 ± 0.04	4.83 ± 0.01	4.84 ± 0.0	4.84 ± 0.0	4.84 ± 0.0	10.57 ± 0.05	10.64 ± 0.0	10.09 ± 0.6
PGD-MOO (Ours)	4.46 ± 0.03	4.84 ± 0.0	4.84 ± 0.0	4.84 ± 0.0	4.84 ± 0.0	10.6 ± 0.01	10.65 ± 0.0	10.51 ± 0.04

E.3 Detailed Results

Table 27: Evaluation of the Δ -spread metric with 256 sampled designs on ZDT subtask, part of the **synthetic** set of tasks. Results are averaged over 5 different random seeds. Lower values are better.

Mothod	7DT1	ZDT2	7DT2	ZDT4	ZDT6
Method	ZDT1	LD12	ZDT3	ZD14	ZDIO
MultiHead-GradNorm	0.96 ± 0.19	0.94 ± 0.16	0.93 ± 0.17	0.79 ± 0.15	0.77 ± 0.16
MultiHead-PcGrad	0.83 ± 0.1	0.98 ± 0.13	0.79 ± 0.03	0.67 ± 0.04	0.82 ± 0.11
MultiHead	1.13 ± 0.08	1.04 ± 0.05	0.83 ± 0.06	0.68 ± 0.03	1.22 ± 0.07
MultipleModels-COM	0.89 ± 0.04	0.79 ± 0.11	0.83 ± 0.05	0.64 ± 0.03	1.0 ± 0.09
MultipleModels-ICT	1.1 ± 0.02	1.01 ± 0.07	0.86 ± 0.06	0.69 ± 0.07	0.98 ± 0.06
MultipleModels-IOM	0.94 ± 0.1	0.9 ± 0.05	0.81 ± 0.07	0.73 ± 0.04	$\textbf{0.46} \pm \textbf{0.1}$
MultipleModels-RoMA	0.64 ± 0.06	0.92 ± 0.1	0.79 ± 0.07	0.69 ± 0.02	0.78 ± 0.06
MultipleModels-TriMentoring	0.86 ± 0.03	0.86 ± 0.06	0.9 ± 0.04	0.73 ± 0.02	0.78 ± 0.06
MultipleModels	1.07 ± 0.06	1.01 ± 0.03	0.84 ± 0.03	0.7 ± 0.05	1.19 ± 0.04
ParetoFlow	1.46 ± 0.03	1.19 ± 0.1	1.46 ± 0.14	1.31 ± 0.1	0.71 ± 0.05
PGD-MOO + DataPruning (Ours)	$\textbf{0.66} \pm \textbf{0.08}$	0.61 ± 0.03	0.6 ± 0.03	$\textbf{0.6} \pm \textbf{0.04}$	0.8 ± 0.05
PGD-MOO (Ours)	0.68 ± 0.07	0.78 ± 0.09	0.65 ± 0.03	0.6 ± 0.03	0.76 ± 0.03

The detailed results are given in Tables 22, 23 and 26 to 29.

Table 23: Evaluation of hypervolume with 256 sampled designs on subsets of the **RE** task. Results are averaged over 5 different random seeds.

Method	RE34	RE35	RE36	RE37	RE41	RE42	RE61
D(best)	9.3	10.08	7.61	5.57	18.27	14.52	97.49
MultiHead-GradNorm	8.47 ± 1.87	9.76 ± 1.3	9.67 ± 0.43	5.67 ± 1.41	17.06 ± 3.82	18.77 ± 2.99	108.01 ± 1.0
MultiHead-PcGrad	10.11 ± 0.0	10.51 ± 0.05	10.17 ± 0.08	6.68 ± 0.06	20.66 ± 0.1	22.57 ± 0.26	108.54 ± 0.23
MultiHead	10.1 ± 0.01	10.49 ± 0.07	10.23 ± 0.03	6.67 ± 0.05	20.62 ± 0.11	22.38 ± 0.35	108.92 ± 0.22
MultipleModels-COM	9.96 ± 0.09	10.55 ± 0.02	9.82 ± 0.35	6.35 ± 0.1	20.37 ± 0.06	17.44 ± 0.71	107.99 ± 0.48
MultipleModels-ICT	10.1 ± 0.0	10.5 ± 0.01	10.29 ± 0.03	6.73 ± 0.0	20.58 ± 0.04	22.27 ± 0.15	108.68 ± 0.27
MultipleModels-IOM	10.11 ± 0.01	10.57 ± 0.01	10.29 ± 0.04	6.71 ± 0.02	20.66 ± 0.05	22.43 ± 0.1	107.71 ± 0.5
MultipleModels-RoMA	9.91 ± 0.01	10.53 ± 0.03	9.72 ± 0.28	6.67 ± 0.02	20.39 ± 0.09	21.41 ± 0.37	108.47 ± 0.28
MultipleModels-TriMentoring	10.08 ± 0.02	10.59 ± 0.0	9.64 ± 1.42	6.73 ± 0.01	20.68 ± 0.04	21.6 ± 0.19	108.61 ± 0.29
MultipleModels	10.11 ± 0.0	10.55 ± 0.01	10.24 ± 0.03	6.73 ± 0.03	20.77 ± 0.08	22.59 ± 0.11	108.96 ± 0.06
ParetoFlow	11.2 ± 0.35	11.12 ± 0.02	8.42 ± 0.35	6.55 ± 0.59	19.41 ± 0.92	20.35 ± 5.31	107.1 ± 6.96
PGD-MOO + Data Pruning (Ours)	9.15 ± 0.11	10.43 ± 0.04	9.48 ± 0.33	5.99 ± 0.18	19.37 ± 0.15	17.4 ± 0.63	103.04 ± 1.71
PGD-MOO (Ours)	9.39 ± 0.16	10.32 ± 0.1	9.37 ± 0.17	6.13 ± 0.12	19.31 ± 0.46	19.01 ± 0.68	105.02 ± 1.14

Table 24: Evaluation of hypervolume with 256 sampled designs on subsets of the **C10MOP** tasks. Results are averaged over 5 different random seeds.

Approach	C10MOP1	C10MOP2	C10MOP3	C10MOP4	C10MOP5	C10MOP6	C10MOP7	C10MOP8	C10MOP9
MultipleModels	1.3858 ± 0.0442	1.3296 ± 0.0300	10.0132 ± 0.2535	21.8476 ± 0.2264	36.8597 ± 2.7523	95.0340 ± 7.5757	362.8160 ± 18.0855	5.2041 ± 0.1013	11.6359 ± 0.4404
MultipleModels-COM	*1.4702 ± 0.0000*	1.3321 ± 0.0054	11.0189 ± 0.0365	23.0747 ± 0.0868	49.7248 ± 0.1496	$*107.0121 \pm 0.7802*$	480.4704 ± 14.0997	5.2402 ± 0.0257	13.9464 ± 0.3804
MultipleModels-ICT	1.3526 ± 0.0150	1.3234 ± 0.0446	9.9906 ± 0.3720	20.2256 ± 0.7048	38.9028 ± 0.4978	95.8324 ± 6.6621	334.2373 ± 41.4124	4.9339 ± 0.0759	12.4803 ± 0.2973
MultipleModels-IOM	1.3746 ± 0.1341	1.2992 ± 0.0603	10.5681 ± 0.1584	21.9670 ± 0.3673	47.6971 ± 0.9712	99.9001 ± 3.1050	436.2843 ± 27.0213	5.1168 ± 0.0708	13.7110 ± 0.4607
MultipleModels-RoMA	1.3660 ± 0.0669	1.3355 ± 0.0251	9.8492 ± 0.3837	21.4023 ± 0.4962	38.4872 ± 3.4435	93.0900 ± 3.6038	357.7016 ± 41.3808	5.0832 ± 0.0801	13.5530 ± 0.2167
MultipleModels-TriMentoring	1.4042 ± 0.0336	1.2416 ± 0.0652	10.0904 ± 0.2997	21.3896 ± 1.0433	40.7722 ± 3.5499	96.7069 ± 4.5694	408.3003 ± 28.6059	4.9647 ± 0.0968	12.7916 ± 0.2853
MultiHead	1.4559 ± 0.0227	1.2746 ± 0.0588	10.2391 ± 0.2114	21.2637 ± 1.2549	36.0405 ± 3.3757	98.8094 ± 0.6955	340.8008 ± 60.0297	5.0691 ± 0.1096	11.4813 ± 0.5663
MultiHead-GradNorm	1.4309 ± 0.0155	1.2636 ± 0.0572	10.0193 ± 0.2474	20.7159 ± 1.0982	30.5653 ± 5.2836	77.9574 ± 11.9034	306.7220 ± 39.5226	5.3211 ± 0.1007	12.9097 ± 0.5352
MultiHead-PcGrad	1.4601 ± 0.0102	1.3023 ± 0.0787	10.2801 ± 0.2455	21.4537 ± 0.6093	38.9828 ± 5.0494	88.2995 ± 9.7358	360.9641 ± 30.9560	4.9822 ± 0.0631	12.6775 ± 0.3565
ParetoFlow	1.4456 ± 0.0171	1.3437 ± 0.0164	10.6091 ± 0.2478	21.6532 ± 0.6013	48.6245 ± 0.8522	104.8361 ± 1.9998	463.2916 ± 21.6113	5.2958 ± 0.0921	$*14.3905 \pm 0.2319*$
PGD-MOO + Data Pruning (Ours)	1.4817 ± 0.0021	1.3817 ± 0.0138	$*11.1524 \pm 0.0165*$	$*23.8769 \pm 0.1086*$	$*49.8578 \pm 0.0266*$	106.6697 ± 0.9115	500.4782 ± 1.7625	5.5659 ± 0.0156	14.4528 ± 0.1726
PGD-MOO (Ours)	1.4511 ± 0.0141	$*1.3598 \pm 0.0105*$	11.1826 ± 0.0148	23.9233 ± 0.0821	49.8683 ± 0.0658	107.2650 ± 0.6335	*499 1712 ± 1 3745*	*5 4807 ± 0 0363*	14.0768 ± 0.2056

Table 25: Evaluation of hypervolume with 256 sampled designs on the **IN1K** tasks. Results are averaged over 5 different random seeds.

Approach	IN1KMOP1	IN1KMOP2	IN1KMOP3	IN1KMOP4	IN1KMOP5	IN1KMOP6	IN1KMOP7	IN1KMOP8	IN1KMOP9
MultipleModels	5.6231 ± 0.0610	6.0828 ± 0.2008	14.3020 ± 0.0576	4.1980 ± 0.0303	4.4503 ± 0.0281	10.6306 ± 0.3082	4.6675 ± 0.1023	9.1011 ± 0.1883	11.2394 ± 0.3227
MultipleModels-COM	5.4126 ± 0.0963	6.1518 ± 0.0568	14.6918 ± 0.1703	4.3015 ± 0.0448	4.5755 ± 0.0157	11.3625 ± 0.2449	5.1201 ± 0.1738	11.3815 ± 0.0824	14.9066 ± 0.1649
MultipleModels-ICT	5.6369 ± 0.0287	6.0640 ± 0.2808	14.3255 ± 0.1601	4.2440 ± 0.0171	4.3804 ± 0.0231	10.9187 ± 0.0799	4.9460 ± 0.0873	9.6489 ± 0.2599	11.6043 ± 0.6310
MultipleModels-IOM	5.5938 ± 0.0890	6.0892 ± 0.2250	14.7332 ± 0.0914	4.1076 ± 0.4522	4.6096 ± 0.0408	10.6794 ± 1.0307	5.1611 ± 0.1263	$*11.1559 \pm 0.2388*$	$*14.6504 \pm 0.6083*$
MultipleModels-RoMA	5.5776 ± 0.0557	6.1352 ± 0.1875	14.3641 ± 0.2001	4.1302 ± 0.0364	3.6911 ± 0.0412	8.0256 ± 0.3621	4.7364 ± 0.1182	9.0267 ± 0.1139	10.6159 ± 0.3216
MultipleModels-TriMentoring	5.4462 ± 0.0192	5.3899 ± 0.0119	14.2874 ± 0.1749	4.3775 ± 0.0281	4.4060 ± 0.0317	10.9430 ± 0.0669	5.0492 ± 0.0850	10.1604 ± 0.3933	11.0185 ± 0.4408
MultiHead	5.6206 ± 0.0161	5.8983 ± 0.1535	14.2471 ± 0.1133	4.1108 ± 0.1259	4.2844 ± 0.0877	10.3601 ± 0.0467	4.8340 ± 0.0840	9.2124 ± 0.1680	10.2314 ± 0.9201
MultiHead-GradNorm	5.1362 ± 0.5426	6.2062 ± 0.0950	14.0209 ± 0.1754	3.1755 ± 0.0474	4.2984 ± 0.6297	8.1613 ± 0.7969	4.6107 ± 0.2090	10.1800 ± 0.6765	11.4468 ± 1.1444
MultiHead-PcGrad	5.5797 ± 0.0810	6.0273 ± 0.3497	14.2122 ± 0.0955	4.2014 ± 0.0729	4.2996 ± 0.0449	10.8542 ± 0.1305	4.8260 ± 0.3493	8.7804 ± 0.2875	10.2910 ± 0.0455
ParetoFlow	5.3459 ± 0.1106	5.9646 ± 0.1658	14.3332 ± 0.2594	4.3161 ± 0.0514	4.6240 ± 0.0506	11.6062 ± 0.0935	4.8707 ± 0.0423	11.1389 ± 0.1251	14.4814 ± 0.1094
PGD-MOO + Data Pruning (Ours)	*5.7570 ± 0.0664*	6.4504 ± 0.0201	$*14.7568 \pm 0.1310*$	$*4.3928 \pm 0.0296*$	$*4.6531 \pm 0.0426*$	$*11.7936 \pm 0.1010*$	5.3022 ± 0.0705	10.6270 ± 0.1074	13.9399 ± 0.2251
PGD-MOO (Ours)	5.7638 ± 0.0489	$*6.4305 \pm 0.0232*$	14.8635 ± 0.1562	4.4924 ± 0.0105	4.7465 ± 0.0146	11.9365 ± 0.0626	$*5.1797 \pm 0.0780*$	10.7654 ± 0.1653	13.6189 ± 0.3393

Table 26: Evaluation of the Δ -spread metric with 256 sampled designs on DTLZ subtask, part of the **synthetic** set of tasks. Results are averaged over 5 different random seeds. Lower values are better.

Method	DTLZ1	DTLZ2	DTLZ3	DTLZ4	DTLZ5	DTLZ6	DTLZ7
MultiHead-GradNorm	0.61 ± 0.03	0.89 ± 0.24	0.88 ± 0.29	0.96 ± 0.14	0.75 ± 0.1	0.95 ± 0.28	1.2 ± 0.18
MultiHead-PcGrad	0.65 ± 0.04	0.73 ± 0.05	0.76 ± 0.11	1.08 ± 0.2	0.77 ± 0.06	0.87 ± 0.06	1.15 ± 0.2
MultiHead	0.86 ± 0.08	0.93 ± 0.15	0.93 ± 0.16	0.98 ± 0.12	0.92 ± 0.14	0.88 ± 0.2	0.93 ± 0.11
MultipleModels-COM	0.69 ± 0.02	0.85 ± 0.15	0.73 ± 0.06	1.09 ± 0.12	0.89 ± 0.08	1.15 ± 0.15	0.78 ± 0.03
MultipleModels-ICT	0.7 ± 0.02	0.79 ± 0.02	0.63 ± 0.1	$\textbf{0.92} \pm \textbf{0.03}$	0.8 ± 0.05	0.91 ± 0.06	0.77 ± 0.05
MultipleModels-IOM	0.66 ± 0.02	0.96 ± 0.18	0.67 ± 0.04	1.23 ± 0.24	0.91 ± 0.07	1.11 ± 0.09	0.75 ± 0.03
MultipleModels-RoMA	0.62 ± 0.03	1.06 ± 0.08	0.89 ± 0.11	1.28 ± 0.08	0.93 ± 0.13	0.76 ± 0.1	0.69 ± 0.03
MultipleModels-TriMentoring	0.72 ± 0.03	0.91 ± 0.1	0.66 ± 0.09	0.95 ± 0.07	0.7 ± 0.06	0.8 ± 0.09	0.81 ± 0.05
MultipleModels	0.88 ± 0.07	1.11 ± 0.26	1.0 ± 0.22	0.93 ± 0.13	0.92 ± 0.17	1.0 ± 0.24	0.85 ± 0.12
ParetoFlow	0.82 ± 0.02	1.07 ± 0.07	0.68 ± 0.09	1.63 ± 0.15	1.04 ± 0.06	1.16 ± 0.09	0.84 ± 0.09
PGD-MOO + Data Pruning (Ours)	$\textbf{0.58} \pm \textbf{0.04}$	0.52 ± 0.03	$\textbf{0.46} \pm \textbf{0.02}$	1.66 ± 0.04	0.51 ± 0.02	0.63 ± 0.02	0.53 ± 0.04
PGD-MOO (Ours)	0.62 ± 0.02	0.5 ± 0.03	$\textbf{0.46} \pm \textbf{0.02}$	1.6 ± 0.04	$\textbf{0.51} \pm \textbf{0.02}$	$\textbf{0.61} \pm \textbf{0.03}$	0.63 ± 0.02

Table 28: Evaluation of the Δ -spread metric with 256 sampled designs on subsets of the **RE** task. Results are averaged over 5 different random seeds. Lower values are better.

Method	RE21	RE22	RE23	RE24	RE25	RE31	RE32	RE33
MultiHead-GradNorm	0.77 ± 0.15	1.61 ± 0.37	1.7 ± 0.35	0.98 ± 0.4	1.54 ± 0.5	0.91 ± 0.17	1.26 ± 0.28	0.92 ± 0.14
MultiHead-PcGrad	0.47 ± 0.04	1.8 ± 0.22	1.14 ± 0.21	1.25 ± 0.4	1.6 ± 0.28	1.05 ± 0.25	1.09 ± 0.13	0.91 ± 0.19
MultiHead	0.42 ± 0.04	1.43 ± 0.22	1.03 ± 0.23	$\textbf{1.13} \pm \textbf{0.19}$	1.86 ± 0.04	$\textbf{0.94} \pm \textbf{0.14}$	$\textbf{0.84} \pm \textbf{0.14}$	1.16 ± 0.05
MultipleModels-COM	0.56 ± 0.12	1.22 ± 0.42	1.2 ± 0.49	1.08 ± 0.23	1.63 ± 0.1	1.24 ± 0.17	1.23 ± 0.19	0.87 ± 0.07
MultipleModels-ICT	0.38 ± 0.02	1.78 ± 0.12	$\textbf{0.84} \pm \textbf{0.07}$	0.67 ± 0.12	1.54 ± 0.04	1.28 ± 0.19	0.91 ± 0.09	1.0 ± 0.24
MultipleModels-IOM	0.98 ± 0.4	1.84 ± 0.08	1.26 ± 0.23	1.58 ± 0.24	1.54 ± 0.25	1.07 ± 0.27	1.09 ± 0.19	0.99 ± 0.06
MultipleModels-RoMA	1.19 ± 0.09	1.57 ± 0.56	1.33 ± 0.49	1.22 ± 0.24	1.44 ± 0.43	1.39 ± 0.27	1.15 ± 0.18	0.89 ± 0.06
MultipleModels-TriMentoring	0.37 ± 0.01	1.73 ± 0.12	0.91 ± 0.15	0.56 ± 0.03	1.35 ± 0.04	1.17 ± 0.14	0.99 ± 0.09	$\textbf{0.85} \pm \textbf{0.03}$
MultipleModels	0.37 ± 0.02	1.85 ± 0.12	0.82 ± 0.46	0.99 ± 0.22	1.72 ± 0.36	1.65 ± 0.22	0.9 ± 0.26	1.16 ± 0.2
ParetoFlow	1.5 ± 0.12	1.37 ± 0.11	-	-	-	1.66 ± 0.03	1.34 ± 0.0	1.07 ± 0.11
PGD-MOO + Data Pruning (Ours)	0.61 ± 0.03	1.29 ± 0.08	1.42 ± 0.11	1.13 ± 0.01	1.12 ± 0.08	1.34 ± 0.28	1.62 ± 0.1	0.83 ± 0.17
PGD-MOO (Ours)	0.61 ± 0.03	$\textbf{1.28} \pm \textbf{0.07}$	1.08 ± 0.06	1.14 ± 0.02	1.17 ± 0.07	1.32 ± 0.15	1.59 ± 0.04	0.89 ± 0.06

Table 29: Evaluation of the Δ -spread metric with 256 sampled designs on subsets of the **RE** task. Results are averaged over 5 different random seeds. Lower values are better.

Method	RE34	RE35	RE36	RE37	RE41	RE42	RE61
MultiHead-GradNorm	0.96 ± 0.23	1.17 ± 0.14	1.19 ± 0.19	1.19 ± 0.51	1.13 ± 0.5	1.12 ± 0.51	0.72 ± 0.05
MultiHead-PcGrad	1.11 ± 0.08	0.99 ± 0.13	0.91 ± 0.17	0.76 ± 0.04	0.62 ± 0.01	0.9 ± 0.08	0.72 ± 0.03
MultiHead	1.18 ± 0.02	1.03 ± 0.06	1.15 ± 0.16	0.76 ± 0.03	0.64 ± 0.02	0.86 ± 0.05	0.74 ± 0.06
MultipleModels-COM	1.16 ± 0.02	0.89 ± 0.03	0.94 ± 0.13	0.73 ± 0.02	0.56 ± 0.02	0.68 ± 0.07	0.66 ± 0.03
MultipleModels-ICT	1.06 ± 0.06	1.09 ± 0.04	1.05 ± 0.04	0.75 ± 0.04	0.61 ± 0.04	0.75 ± 0.04	0.65 ± 0.05
MultipleModels-IOM	1.09 ± 0.05	1.03 ± 0.06	1.15 ± 0.05	0.67 ± 0.04	0.57 ± 0.02	0.73 ± 0.06	0.62 ± 0.08
MultipleModels-RoMA	1.02 ± 0.03	1.22 ± 0.07	0.93 ± 0.13	0.71 ± 0.02	0.59 ± 0.01	0.66 ± 0.05	0.59 ± 0.05
MultipleModels-TriMentoring	1.05 ± 0.14	0.82 ± 0.11	1.2 ± 0.24	0.74 ± 0.02	0.58 ± 0.01	0.78 ± 0.07	0.63 ± 0.05
MultipleModels	1.22 ± 0.03	1.07 ± 0.12	1.03 ± 0.07	0.82 ± 0.03	0.62 ± 0.04	0.83 ± 0.08	0.7 ± 0.06
ParetoFlow	0.88 ± 0.05	1.13 ± 0.02	1.05 ± 0.02	1.12 ± 0.1	1.11 ± 0.07	0.9 ± 0.1	0.68 ± 0.02
PGD-MOO + Data Pruning (Ours)	0.58 ± 0.05	$\textbf{0.67} \pm \textbf{0.04}$	0.7 ± 0.05	$\textbf{0.44} \pm \textbf{0.03}$	0.42 ± 0.0	$\textbf{0.49} \pm \textbf{0.03}$	$\textbf{0.52} \pm \textbf{0.03}$
PGD-MOO (Ours)	0.56 ± 0.02	0.9 ± 0.12	0.64 ± 0.04	0.5 ± 0.01	0.43 ± 0.02	0.49 ± 0.04	0.58 ± 0.04